

Unveiling the sea: universality of the transverse momentum dependent quark distributions at small x

Paul Caucal,^{1,*} Marcos Guerrero Morales,^{2,†} Edmond Iancu,^{3,‡} Farid Salazar,^{2,4,5,6,§} and Feng Yuan^{7,3,¶}

¹SUBATECH UMR 6457 (IMT Atlantique, Université de Nantes, IN2P3/CNRS), 4 rue Alfred Kastler, 44307 Nantes, France

²Department of Physics, Temple University, Philadelphia, PA 19122 - 1801, USA

³Université Paris-Saclay, CNRS, CEA, Institut de physique théorique, F-91191, Gif-sur-Yvette, France

⁴RIKEN-BNL Research Center, Brookhaven National Laboratory, Upton, New York 11973, USA

⁵Physics Department, Brookhaven National Laboratory, Upton, New York 11973, USA

⁶Institute for Nuclear Theory, University of Washington, Seattle WA 98195-1550, USA

⁷Nuclear Science Division, Lawrence Berkeley National Laboratory, Berkeley, CA 94720, USA

Within the Colour Glass Condensate effective theory, we demonstrate that back-to-back dijet correlations in dilute-dense collisions involving a small- x quark from the nuclear target can be factorised in terms of universal transverse momentum dependent distributions (TMDs) for the sea quarks. Two building blocks are needed to construct all these TMDs at the operator level: the sea quark TMD operator which appears in semi-inclusive Deep-Inelastic Scattering (SIDIS) or in the Drell-Yan process and the elastic S -matrix for a quark-antiquark dipole. Compared to SIDIS, the saturation effects are stronger for dijet production in forward proton-nucleus collisions, due to additional scattering in the initial and final state, effectively resulting in a larger value for the nuclear saturation momentum.

Introduction. One of the key insights from the high-energy electron-proton collisions at HERA is the rapid rise of the gluon distribution in protons as the longitudinal momentum fraction x of the gluon with respect to the proton decreases [1]. This steep growth is moderated by non-linear gluon saturation, an emergent phenomenon described by the Colour Glass Condensate (CGC) effective theory [2–6]. The experimental characterisation of gluon saturation is a central objective of the future Electron-Ion Collider (EIC) [7–9], which will extend the groundbreaking work of HERA [10, 11]. On the other hand, HERA also showed [12, 13] that the proton wave-function at small x contains a substantial component of “sea” quarks, which arise primarily from quark-antiquark pair production from small- x gluons. In this Letter, we demonstrate that the CGC consistently accounts for the sea quark contribution [14–16] inside nuclei and predicts the shape of the quark transverse momentum dependent (TMD) distributions [17, 18] in the saturation regime.

Our analysis builds upon pioneering work which unveiled sea quark TMD factorisation for selected processes in electron-nucleus (eA) deep inelastic scattering (DIS) at small x : the semi-inclusive production (SIDIS) of quark jets (or hadrons) [19–21], lepton-jet correlations [22], and the diffractive production of quark jets [23] and of quark-gluon dijets [24]. Despite such interesting, but rare, examples, a systematic understanding of the emergence of quark TMD factorisation at small x — similar to that for the case of gluons [25–50] — was still missing. It is our purpose in this Letter to fill this gap. Via the study of representative processes describing inclusive two-particle production (dijets, dihadrons, or photon-jets, to be collectively referred to as “dijets” in what follows) in eA DIS and proton-nucleus (pA) collisions,

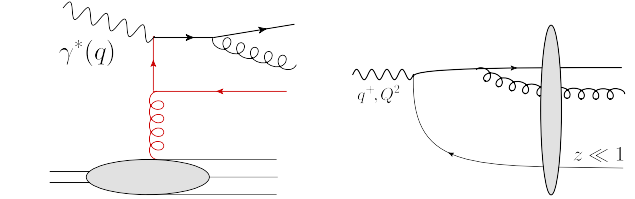


Figure 1. Graphs contributing to quark-gluon production in DIS at small x and to leading order. Left: target picture (photon absorbed by a sea quark). Right: CGC picture (a $q\bar{q}g$ fluctuation of the photon scatters off the shockwave target field).

we will demonstrate the ubiquitousness and the universality of the sea quark TMDs, as computed from the CGC.

The dijet processes of interest for us here involve a hard scattering between a parton from the dilute projectile and a sea quark with $x \ll 1$ from the nuclear target, hence they are suppressed by a power of the QCD coupling α_s compared to gluon-mediated processes leading to similar final states. Yet, since the sea quark distribution is driven by that of the small- x gluons, these processes show exactly the same behaviour at high energy as their gluonic counterparts. So, their contributions must be taken into account for the phenomenology of back-to-back two-particle correlations at high energies, as probed via forward particle production in pA collisions at the Large Hadron Collider, or in eA collisions at the EIC. Since the sea quark TMD is sensitive to gluon saturation [14–16] (see also below), our results open a new window for saturation studies at colliders through the quark channel.

To be more specific, consider quark-gluon dijet production in DIS, as illustrated (within the standard par-

ton picture for the target) by the left Feynman graph in Fig. 1. The dijets are assumed to be hard and nearly back-to-back in the transverse plane: their relative transverse momentum P_\perp is much larger than both their momentum imbalance K_\perp and the target saturation momentum $Q_s(x)$. Despite being hard, the dijets can probe low- x partons in the target wavefunction provided the center-of-mass (COM) energy is sufficiently high and that, in the COM frame, the jets are produced at forward rapidities, in the fragmentation region of the dilute projectile.

Below, we shall compute the dijet cross-section in the CGC effective theory, to leading order (LO) in α_s and to leading powers (LP) in the small ratios K_\perp/P_\perp and Q_s/P_\perp . We shall thus find *TMD factorisation*: to the accuracy of interest, the cross-section is the product between a *hard factor* (the same as for the corresponding processes at moderate x , see e.g. [51]) and a *sea quark TMD*, for which the CGC approach offers explicit results from first principles.

As we shall see, there are multiple such sea quark TMDs, depending upon the process. Yet, they share a universal structure determined by the colour flow of the hard partonic process. At the operator level, this universal structure reflects the various possible gauge links connecting bilocal quark field operators [52]. In the multicolour limit $N_c \rightarrow \infty$, all the emerging TMDs are built with only two ingredients: the sea quark TMD from the CGC calculation of SIDIS [19] and a colour dipole operator describing initial-state and final-state interactions in the eikonal approximation.

Target vs. projectile picture. TMD (or collinear) factorisation is traditionally formulated in the target parton picture, where the small- x quark that is knocked out by the collision is a constituent of the target — the quark component of a sea quark-antiquark ($q\bar{q}$) pair. The CGC picture is however different. The target is described as a classical colour field (a “shockwave”) representing the small- x gluons, but there are no explicit quark degrees of freedom: valence quarks are implicitly included as sources for the colour fields, but the sea quarks are absent¹. In the CGC picture, the would-be *scattering* between a parton from the projectile and a sea quark from the target is instead described as the *emission* of a soft *antiquark* by the projectile parton. This antiquark participates in the scattering with the target colour field, but it is not measured in the final state. Thus, the CGC calculation of dijet production requires the study of a three-parton Fock component of the light-cone (LC) wavefunction (WF) of the projectile (see the right graph

in Fig. 1 for an example). To that aim, the calculation should be performed in a Lorentz frame where the projectile is ultrarelativistic and in the projectile LC gauge.

Let us consider the DIS process in Fig. 1 for definiteness. The CGC factorisation for this process, a.k.a. the colour dipole picture (CDP) [56–59], is formulated in a frame where the virtual photon is a right-mover with 4-momentum $q^\mu = (q^+, q^- = -Q^2/2q^+, \mathbf{0}_\perp)$ with $q^+ \gg Q$, while the nuclear target is a left mover with $P_N^\mu \simeq \delta^\mu - P_N^-$ per nucleon. The photon LCWF is constructed in perturbation theory, in the LC gauge $A_a^+ = 0$. To compute quark-gluon (qg) dijet production to LO, one needs the 3-parton Fock state $q\bar{q}g$. Introducing LC longitudinal momenta $k_i^+ \equiv z_i q^+$ and transverse momenta \mathbf{k}_i for the three partons ($i = q, \bar{q}, g$), the dijet transverse relative momentum and imbalance are defined as $\mathbf{P} = z_g \mathbf{k}_q - z_q \mathbf{k}_g$ and $\mathbf{K} = \mathbf{k}_q + \mathbf{k}_g$, respectively, with $K_\perp \ll P_\perp$ in the back-to-back limit. To simplify notations, we shall use z and \mathbf{k} (instead of $z_{\bar{q}}, \mathbf{k}_{\bar{q}}$) for the unmeasured antiquark.

To uncover TMD factorisation for qg dijets, we isolate the LP in the ratio K_\perp/P_\perp and integrate out the kinematics (z, \mathbf{k}) of the unmeasured antiquark. This integration is controlled by transverse momenta $k_\perp \sim K_\perp$ and small values $z \sim K_\perp^2/P_\perp^2 \ll 1$ for the longitudinal momentum fraction. This can be understood from a formation time argument: in a hard process, the antiquark formation time $\Delta x^+ \sim zq^+/k_\perp^2$ is comparable to that of the hard qg pair:

$$\frac{zq^+}{K_\perp^2} \sim \frac{z_q z_g q^+}{P_\perp^2} \Rightarrow z \sim \frac{K_\perp^2}{P_\perp^2}. \quad (1)$$

Thus, importantly, the unmeasured antiquark in the CGC picture (the same as the struck sea quark in the target picture) is *soft* both w.r.t. to the projectile, $z \ll 1$, and w.r.t. the target, $x \ll 1$. Being soft, it can indeed be “transferred” between the projectile and the target, as explained in [21, 24, 42, 49, 50, 60].

This special kinematics for the three parton system also implies a special geometry for the collision in the transverse plane, as suggested by our drawing of the CGC graph in Fig. 1: the hard qg pair has a small size $r \sim 1/P_\perp \ll 1/Q_s$ and is separated from the soft antiquark by a large distance $R \sim 1/K_\perp \gg r$. Accordingly, the incoming photon, the intermediate quark, and the hard qg dijet are all aligned with each other: the respective transverse coordinates are roughly the same.

Quark-gluon dijet production in eA DIS. Let us now compute the cross-section for the CGC process $\gamma^* + A \rightarrow qg(\bar{q}) + X$. In general, there are two possible topologies: gluon emission by the quark (cf. Fig. 1), or by the antiquark (see Fig. 2). For a photon with transverse polarisation (γ_T^*), both topologies contribute on the same footing, but for a longitudinal one (γ_L^*), the first possibility is suppressed. (Indeed, in that case, the photon splitting

¹ Fermionic background fields can be introduced via sub-eikonal corrections to the scattering. This has been used to study quark TMD factorisation in dilute-dense collisions [53–55]. In this approach, the quark TMDs are not explicitly computed, but merely related to formal correlation functions of the fermionic background field.

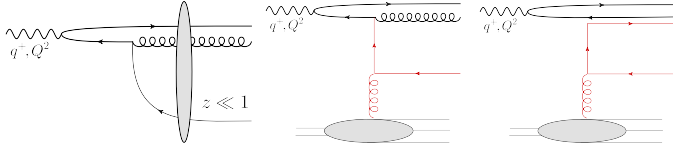


Figure 2. Left: CGC picture for back-to-back quark-gluon dijets in $\gamma_L^* A$ collisions. Middle: The corresponding target picture. Right: The associated colour flow at large N_c .

function $\gamma_L^* \rightarrow q\bar{q}$ is proportional to $z(1-z) \ll 1$.) For simplicity, we present details only for γ_L^* and refer the reader to the Supplemental Material for the discussion of γ_T^* .

To LP in K_\perp/P_\perp , the amplitude for gluon emission by the antiquark is obtained as

$$\mathcal{M}_{qg(\bar{q})}^{\lambda\sigma\bar{\sigma},a} = 8ee_f g \sqrt{z_q z_{\bar{q}}} q^+ \delta^{\sigma,-\bar{\sigma}} \delta^{\lambda\sigma} \frac{Q}{M_{qg}^2 + Q^2} \quad (2)$$

$$\times \int \frac{d^2\ell}{(2\pi)^2} \frac{\ell \cdot \epsilon^{\lambda*}}{\ell^2 + z(Q^2 + M_{qg}^2)} C_1^a(\mathbf{K} - \ell, \ell + \mathbf{k}),$$

where $M_{qg}^2 \equiv (k_q + k_g)^2 \simeq P_\perp^2/(z_q z_g)$, $\bar{\lambda}$ and a refer to the transverse polarisation and the colour of the produced gluon, σ and $\bar{\sigma}$ are helicity indices for the quark and antiquark, g and e denote the strong and electromagnetic charges, and e_f is the fractional electric charge of a quark with flavour f . Eq. (2) involves the colour operator

$$C_1^a(\mathbf{q}_1, \mathbf{q}_2) = \int_{x,y} e^{-iq_1 \cdot x - iq_2 \cdot y} t^a [V_x V_y^\dagger - 1], \quad (3)$$

with V_x a light-like Wilson line in the fundamental representation of $SU(N_c)$ with fixed transverse coordinate x . The Wilson lines in Eq. (3) describe the scattering of the effective $q\bar{q}$ dipole, where the “quark” truly is the small qg pair. The colour matrix t^a refers to the gluon emission. By removing this matrix and replacing $g \rightarrow -ee_f$ in Eq. (2), one gets the amplitude for $\gamma q\bar{q}$ production in DIS; hence this paragraph also encompasses γ -jet correlations in DIS [61].

To get the quark-gluon dijet cross-section, one must square this amplitude and integrate over the soft antiquark phase space, i.e. over \mathbf{k} and z . After also extracting the LP in K_\perp/P_\perp , one finds

$$\frac{d\sigma \gamma_L^* A \rightarrow qg + X}{d^2\mathbf{P} d^2\mathbf{K} dz_q dz_g} = \delta(1 - z_q - z_g) \frac{8\alpha_{\text{em}} e_f^2 \alpha_s Q^2}{z_g (Q^2 + M_{qg}^2)^3} \quad (4)$$

$$\times C_F x q^{(1)}(x, \mathbf{K}).$$

This result is leading twist since the hard factor in the first line behaves like $1/P_\perp^4$ when $P_\perp^2 \sim Q^2$. As expected, this is the same as the hard factor in the collinear factorisation result for the partonic process $\gamma_L^* q \rightarrow qg$.

Eq. (4) demonstrates TMD factorisation with an explicit result for the sea quark TMD, conveniently written

as $xq^{(1)}(x, \mathbf{K}) \equiv \langle \mathcal{Q}(\mathbf{K}) \rangle_x$, where the brackets $\langle \dots \rangle_x$ refer to the CGC average over the target colour fields and the sea quark operator \mathcal{Q}

$$\mathcal{Q}(\mathbf{K}) \equiv \frac{N_c}{4\pi^4} \int_{\mathbf{b}, \mathbf{q}} \mathcal{D}_F^{(1)}(\mathbf{b}, \mathbf{q}) \quad (5)$$

$$\times \left[1 - \frac{\mathbf{K} \cdot (\mathbf{K} - \mathbf{q})}{K_\perp^2 - (\mathbf{K} - \mathbf{q})^2} \ln \left(\frac{K_\perp^2}{(\mathbf{K} - \mathbf{q})^2} \right) \right],$$

involves the dipole operator $\mathcal{D}_F^{(n=1)}(\mathbf{b}, \mathbf{q})$, defined as (for arbitrary integer n , for later convenience)

$$\mathcal{D}_F^{(n)}(\mathbf{b}, \mathbf{q}) \equiv \int_{\mathbf{r}} \frac{e^{-i\mathbf{q} \cdot \mathbf{r}}}{(2\pi)^2} \left(\frac{1}{N_c} \text{Tr} [V_{\mathbf{b}+\mathbf{r}/2} V_{\mathbf{b}-\mathbf{r}/2}^\dagger] \right)^n. \quad (6)$$

This operator depends upon the impact parameter \mathbf{b} of the $q\bar{q}$ dipole and the transverse momentum \mathbf{q} transferred by the target via the collision. Transverse momentum conservation shows that the difference $\mathbf{q} - \mathbf{K}$ is the momentum of the unmeasured antiquark.

The x dependence of the quark TMD $xq^{(1)}(x, \mathbf{K})$ is controlled by the BK/JIMWLK [62–70] evolution of $\mathcal{D}_F^{(1)}$ down to $x = x_{qg}$, with x_{qg} the target longitudinal fraction taken by the measured dijet. This is obtained from the condition of LC energy (k^-) conservation as $x_{qg} = (M_{qg}^2 + Q^2)/\hat{s}$ with $\hat{s} = (P + q)^2$.

The quark TMD $xq^{(1)}(x, \mathbf{K})$ is identical to that obtained in the CGC calculation of SIDIS at small x [19, 20]. This is consistent with the fact that the colour flow is identical for both processes, due to the small transverse size of the hard dijet. This flow is illustrated in Fig. 2 in the large N_c limit. (The $q\bar{q}$ dipole which is disconnected from the quark TMD has a negligible transverse size $r \sim 1/P_\perp$, so it does not contribute to the colour flow.) Eq. (5) has a natural interpretation in the target picture [71]: \mathbf{q} is the transverse momentum of the parent gluon which generates the $q\bar{q}$ sea pair, while

$$xG^{(2)}(x, \mathbf{q}) \equiv \frac{q_\perp^2 N_c}{2\pi^2 \alpha_s} \int_{\mathbf{b}} \langle \mathcal{D}_F^{(1)}(\mathbf{b}, \mathbf{q}) \rangle_x, \quad (7)$$

represents the dipole unintegrated gluon distribution (UGD). As discussed in [25, 26], this distribution plays the role of a TMD for small- x processes which involve both initial-state and final-state interactions, i.e. which feature coloured partons on both the incoming and the outgoing legs. Of course, this is not the case in DIS, where all the coloured partons are outgoing. Yet, the dipole UGD is relevant in this context since the gluon distribution of the target is “probed” by a $q\bar{q}$ sea pair and the antiquark in this pair mimics an incoming quark in the initial state. This suggests that the second line of Eq. (5) times α_s/q_\perp^2 can be interpreted as a *transverse momentum dependent gluon-to-quark splitting function* (integrated over the splitting fraction ξ). It indeed coincides with the off-shell splitting function employed in k_T -factorisation [72–75]. A more complete result, where the ξ -dependence is visible, can be found in [20, 71].

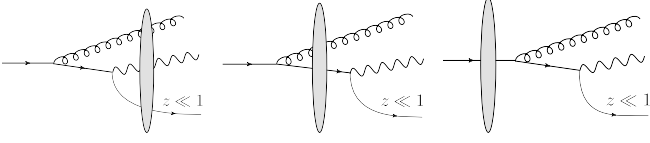


Figure 3. Feynman graphs for $qA \rightarrow \gamma g(q) + X$ amplitudes at small x in the CGC ($\gamma \leftrightarrow g$ exchanged diagrams not shown).

Photon-quark dijets in quark-initiated pA collisions. We now consider inclusive back-to-back photon-jet production in forward pA collisions in the channel $qA \rightarrow \gamma g(q) + X$. That is, the scattering is initiated by a quark from the proton (assumed to be on-shell prior to the collision) and the hadronic “jet” in the final state corresponds to a gluon — so the final quark (with kinematical variables z and \mathbf{k}) is soft and unmeasured: $k_\perp \sim K_\perp$ and $z \sim K_\perp^2/P_\perp^2 \ll 1$. The relevant CGC amplitudes are shown in Fig. 3. As before, the total amplitude drastically simplifies after keeping only the LP in K_\perp/P_\perp , and reads

$$\begin{aligned} \mathcal{M}_{\gamma g(q)}^{\bar{\lambda}\lambda\sigma\sigma'} &= 8ee_f g \sqrt{z} q^+ \delta^{\sigma\sigma'} \delta^{\sigma,-\lambda} \left[\delta^{\lambda\bar{\lambda}} + z_\gamma \delta^{\lambda,-\bar{\lambda}} \right] \\ &\times \frac{\mathbf{P} \cdot \boldsymbol{\epsilon}^{\bar{\lambda}*}}{P^2} \int \frac{d^2\ell}{(2\pi)^2} \left[\frac{\ell \cdot \boldsymbol{\epsilon}^{\lambda*}}{\ell^2 + zM_{\gamma g}^2} + \frac{\mathbf{k} \cdot \boldsymbol{\epsilon}^{\lambda*}}{\mathbf{k}^2 + zM_{\gamma g}^2} \right] \\ &\times C_2^a(\ell + \mathbf{k}, \mathbf{K} - \ell) + (\gamma \leftrightarrow g), \end{aligned} \quad (8)$$

where $\sigma, \sigma', \lambda, \bar{\lambda}$ respectively refer to the incoming and outgoing quark helicities and to the photon and gluon polarisation, a to the colour of the gluon, and $M_{\gamma g}$ is the γ -jet invariant mass. The first (second) term inside the square brackets corresponds to gluon emission before (after) the shockwave. In the first case, the gluon participates in the scattering as well, so the respective amplitude involves the colour operator

$$C_2^a(\mathbf{q}_1, \mathbf{q}_2) = \int_{\mathbf{x}, \mathbf{z}} e^{-i\mathbf{q}_1 \cdot \mathbf{x} - i\mathbf{q}_2 \cdot \mathbf{z}} V_{\mathbf{x}} t^b U_{\mathbf{z}}^{ab}, \quad (9)$$

(with $U_{\mathbf{z}}^{ab}$ an adjoint Wilson line) describing the scattering of quark-gluon system off the strong gluon field of the target. For the second term, the integral over ℓ yields a δ -function enforcing $\mathbf{x} = \mathbf{z}$ which simplifies the colour operator as follows $V_{\mathbf{x}} t^b U_{\mathbf{z}}^{ab} \rightarrow t^a V_{\mathbf{x}}$; as expected, this describes the scattering of the quark probe alone.

Squaring this amplitude and integrating over the kinematic (z, \mathbf{k}) of the unmeasured quark gives the inclusive γ +gluon-jet cross-section in the leading-twist approximation of interest

$$\begin{aligned} \frac{d\sigma^{qA \rightarrow \gamma g + X}}{d^2\mathbf{P} d^2\mathbf{K} dz_\gamma dz_g} &= \delta(1 - z_\gamma - z_g) \frac{\alpha_{\text{em}} e_f^2 \alpha_s}{N_c} \frac{(z_\gamma^2 + z_g^2)}{P^4} \\ &\times \left[\frac{N_c}{2} xq^{(2)}(x, \mathbf{K}) - \frac{1}{2N_c} xq^{(1)}(x, \mathbf{K}) \right], \end{aligned} \quad (10)$$

where $x = x_{\gamma g}$. The first term, which is the only one to survive at large N_c , features a new quark TMD operator

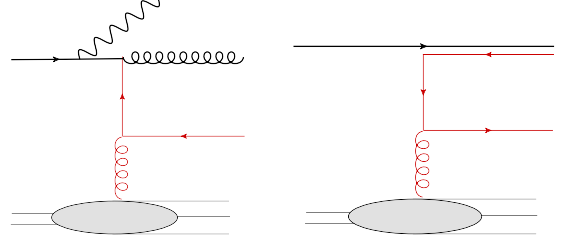


Figure 4. Left: Target picture for γg jets in pA collisions. Right: The associated colour flow at large N_c .

at small x , defined as a convolution between our previous sea quark TMD operator $\mathcal{Q}(\mathbf{b}, \mathbf{K})$ (the version of the operator in Eq. (5) at a fixed value of the impact parameter \mathbf{b}) and the dipole operator $\mathcal{D}_F^{(1)}(\mathbf{b}, \mathbf{q})$ (cf. Eq. (130)):

$$xq^{(2)}(x, \mathbf{K}) = \int_{\mathbf{b}, \mathbf{q}} \left\langle \mathcal{D}_F^{(1)}(\mathbf{b}, \mathbf{q}) \mathcal{Q}(\mathbf{b}, \mathbf{K} - \mathbf{q}) \right\rangle_x. \quad (11)$$

The target picture for this process and the associated colour flow at large N_c are illustrated in Fig. 4. These figures make clear that the overall process involves both initial and final state interactions. After replacing the gluon by a point-like $q\bar{q}$ pair (as appropriate at large N_c), the ensemble of these interactions can be resummed into a fundamental Wilson line extending from $x^+ \rightarrow -\infty$ to $x^+ \rightarrow \infty$, which factorises from the rest of the amplitude. This infinite Wilson line has a fixed transverse coordinate since the incoming quark and the outgoing gluon have roughly the same transverse positions. Its product with the hermitian conjugate Wilson line from the complex conjugate amplitude yields the dipole operator visible in Eq. (11). This can be recognised as a *Wilson loops* (since the transverse fields vanish at $x^+ \rightarrow \pm\infty$), whose appearance was to be expected: such Wilson loop are well known to enter the gauge link structure of the operators defining quark TMDs in processes with both initial and final state interactions [52].

Gluon-quark dijets in gluon-initiated pA collisions. Our last example refers to gluon-quark dijets in pA collisions via the $gq \rightarrow gq$ hard process, which in the CGC calculation looks like $g + A \rightarrow qg(\bar{q}) + X$.

Besides the DIS-like diagrams where the gluon is emitted by the quark or the antiquark, cf. Figs. 1 and 2, there is an additional topology which involves the triple gluon vertex, see Fig. 5. At large N_c , there are two patterns for the colour flow associated with this topology: one where the quark component of the incoming gluon is transmitted to the outgoing gluon, and one where this component becomes the produced quark. In both cases, this quark component gives rise to an infinite Wilson line which generates a Wilson loop (or dipole correlator) in the cross-section. In the second pattern though, there is another such a Wilson line, associated with the antiquark component of the original gluon. Hence, the

cross-section generated by this topology will feature two types of sea quark TMDs: one with a single Wilson loop, as shown in Eq. (11), and another one involving two Wilson loops which in the transverse plane lie on top of each other. (Indeed, in the approximations of interest, the incoming gluon and the two produced jets roughly have the same transverse coordinate.)

The colour flows depicted in Fig. 5 also reveals an interesting structure for the sea quark operator. In the first pattern, the (effective) colour flow corresponds to *initial-state interactions*; hence, the corresponding version of the operator $\mathcal{Q}(\mathbf{b}, \mathbf{K})$ is the one that would naturally enter the Drell-Yan process ($q\bar{q} \rightarrow \gamma^* \rightarrow \ell^+ \ell^- + X$) in pA collisions [20]. For an unpolarised target, this coincides with the respective SIDIS operator in Eq. (5). In the second pattern, we recover the original SIDIS operator $\mathcal{Q}(\mathbf{b}, \mathbf{K})$, with a colour flow encoding final-state interactions.

The total amplitude at LP in K_\perp/P_\perp taking into account all topologies can be found in the Supplemental Material. The final CGC result for the back-to-back qg dijet cross-section is found as (in the large N_c limit)

$$\frac{d\sigma^{gA \rightarrow gq+X}}{d^2\mathbf{P} d^2\mathbf{K} dz_q dz_g} = \delta(1 - z_q - z_g) \frac{\alpha_s^2(1 + z_g^2)}{2z_q \mathbf{P}^4} \times \left[xq^{(3)}(x, \mathbf{K}) + z_g^2 xq^{(2)}(x, \mathbf{K}) \right], \quad (12)$$

where the quark TMDs are defined for generic integer $n \geq 1$ by the following generalisation of Eq. (11):

$$xq^{(n)}(x, \mathbf{K}) = \int_{\mathbf{b}, \mathbf{q}} \left\langle \mathcal{D}_F^{(n-1)}(\mathbf{b}, \mathbf{q}) \mathcal{Q}(\mathbf{b}, \mathbf{K} - \mathbf{q}) \right\rangle_x. \quad (13)$$

Numerical study. We conclude this Letter with a numerical study of the sea quark TMDs at small x , with particular emphasis on $xq^{(2)}$ and $xq^{(3)}$ that have never been considered before. We rely on the mean field (or large- N_c) approximation, which allows us to factorise the CGC average in Eq. (13): $\langle \mathcal{D}_F^{(n)} \mathcal{Q} \rangle \approx \langle \mathcal{D}_F^{(n)} \rangle \langle \mathcal{Q} \rangle$. The basic building block is the dipole correlator, for which we use the McLerran-Venugopalan model [76, 77]. To study nuclear effects, we compare two types of targets: a dilute one (“proton”) with saturation momentum $Q_{s0}^2 = 0.2 \text{ GeV}^2$ and a dense one (“nucleus”) with $Q_s^2 = A^{1/3} Q_{s0}^2 = 1 \text{ GeV}^2$, hence $A^{1/3} = 5$. Our results are presented in Fig. 6, with solid lines for a “nucleus” and dashed lines for a “proton”, and for $n = 1, 2, 3$. As visible in these plots, the TMDs display a universal behaviour at large K_\perp featuring a perturbative power tail $1/K_\perp^2$. On the other hand, they saturate to different values at low momenta $K_\perp \lesssim Q_s$. The saturation region extends with increasing the power n . This is best seen in the nucleus over proton ratio (normalised by $A^{1/3}$) shown in the bottom plot: increasing n effectively yields a larger saturation scale and also a stronger deviation of the ratio from 1. This trend can be analytically understood from Eq. (13): for large $q_\perp \gg Q_s$, the dipole correlator is rapidly decaying, $\langle \mathcal{D}_F^{(n)}(\mathbf{q}) \rangle \propto 1/q_\perp^4$, while it is

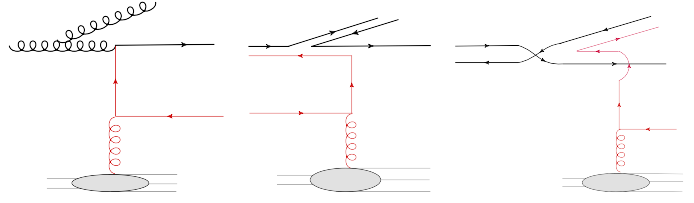


Figure 5. Target picture and large- N_c colour flow for qg jets in gluon-initiated pA collisions: gluon emission by the gluon.

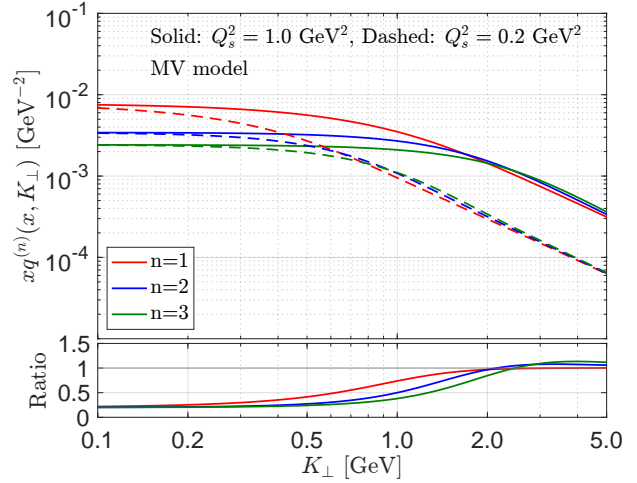


Figure 6. Small- x quark TMD distributions for a proton and a nucleus with $A^{1/3} = 5$. Details in text.

roughly flat in the saturation region $q_\perp^2 \lesssim nQ_s^2$. Hence the integral in Eq. (13) is controlled by $q_\perp^2 \lesssim nQ_s^2$ and this region extends when increasing n .

Conclusion. We have proven sea quark TMD factorisation for various back-to-back dijet processes at high energy from the CGC. The sea quark TMDs have a universal structure, which is built from the fundamental sea quark TMD involved in SIDIS/Drell-Yan at small x and the quark-antiquark dipole correlator. This structure agrees with the gauge link structure of the quark TMDs depending on the underlying hard partonic process, and in particular on the color flow of the external legs not attached to the TMD. These results pave the way towards the systematic incorporation of sea quark effects in the correlation limit of small x processes, a feature which has been largely overlooked in phenomenological works so far. For applications to the phenomenology, it is important to also take into account the additional, soft gluon radiation in the final state, which could strongly modify the back-to-back two-particle correlations. This can be done with the help of the Sudakov resummation method as developed in the CGC formalism [20, 21, 50, 71, 78–85] or, alternatively, by coupling to parton showers [86–88].

Acknowledgements. We are grateful to Xiaoxuan Chu, Larry McLerran, Yacine Mehtar-Tani, Al Mueller,

Björn Schenke and Raju Venugopalan for discussions. We thank the France-Berkeley-Fund from University of California at Berkeley for support. F.S. is supported by the Laboratory Directed Research and Development of Brookhaven National Laboratory and RIKEN- BNL Research Center. Part of this work was conducted while F.S. was supported by the Institute for Nuclear Theory's U.S. DOE under Grant No. DE-FG02-00ER41132. This work is supported in part by the U.S. Department of Energy, Office of Science, Office of Nuclear Physics, under contract number DE-AC02-05CH11231 (F.Y.), under the umbrella of the Quark-Gluon Tomography (QGT) Topical Collaboration with Award DE-SC0023646. P.C., E.I. and F.S. are grateful for the support of the Saturated Glue (SURGE) Topical Theory Collaboration, funded by the U.S. Department of Energy, Office of Science, Office of Nuclear Physics.

* caucal@subatech.in2p3.fr

† marcos.guerrero.morales@temple.edu

‡ edmond.iancu@ipht.fr

§ farid.salazar@temple.edu

¶ fyuan@lbl.gov

- [1] M. Derrick *et al.* (ZEUS), *Phys. Lett. B* **316**, 412 (1993).
- [2] E. Iancu, A. Leonidov, and L. McLerran, in *Cargese Summer School on QCD Perspectives on Hot and Dense Matter* (2002) pp. 73–145, [arXiv:hep-ph/0202270](#).
- [3] E. Iancu and R. Venugopalan, “The Color glass condensate and high-energy scattering in QCD,” in *Quark-gluon plasma 4*, edited by R. C. Hwa and X.-N. Wang (2003) pp. 249–3363, [arXiv:hep-ph/0303204](#).
- [4] F. Gelis, E. Iancu, J. Jalilian-Marian, and R. Venugopalan, *Ann. Rev. Nucl. Part. Sci.* **60**, 463 (2010), [arXiv:1002.0333 \[hep-ph\]](#).
- [5] Y. V. Kovchegov and E. Levin, *Quantum Chromodynamics at High Energy*, Vol. 33 (Oxford University Press, 2013).
- [6] A. Morreale and F. Salazar, *Universe* **7**, 312 (2021), [arXiv:2108.08254 \[hep-ph\]](#).
- [7] A. Accardi *et al.*, *Eur. Phys. J. A* **52**, 268 (2016), [arXiv:1212.1701 \[nucl-ex\]](#).
- [8] R. Abdul Khalek *et al.*, *Nucl. Phys. A* **1026**, 122447 (2022), [arXiv:2103.05419 \[physics.ins-det\]](#).
- [9] P. Achenbach *et al.*, *Nucl. Phys. A* **1047**, 122874 (2024), [arXiv:2303.02579 \[hep-ph\]](#).
- [10] A. M. Stasto, K. J. Golec-Biernat, and J. Kwiecinski, *Phys. Rev. Lett.* **86**, 596 (2001), [arXiv:hep-ph/0007192](#).
- [11] C. Marquet and L. Schoeffel, *Phys. Lett. B* **639**, 471 (2006), [arXiv:hep-ph/0606079](#).
- [12] J. Breitweg *et al.* (ZEUS), *Eur. Phys. J. C* **7**, 609 (1999), [arXiv:hep-ex/9809005](#).
- [13] C. Adloff *et al.* (H1), *Nucl. Phys. B* **497**, 3 (1997), [arXiv:hep-ex/9703012](#).
- [14] L. D. McLerran and R. Venugopalan, *Phys. Rev. D* **59**, 094002 (1999), [arXiv:hep-ph/9809427](#).
- [15] A. H. Mueller, *Nucl. Phys. B* **558**, 285 (1999), [arXiv:hep-ph/9904404](#).
- [16] R. Venugopalan, *Acta Phys. Polon. B* **30**, 3731 (1999), [arXiv:hep-ph/9911371](#).
- [17] J. Collins, *Foundations of Perturbative QCD*, Cambridge Monographs on Particle Physics, Nuclear Physics and Cosmology, Vol. 32 (Cambridge University Press, 2023).
- [18] R. Boussarie *et al.*, (2023), [arXiv:2304.03302 \[hep-ph\]](#).
- [19] C. Marquet, B.-W. Xiao, and F. Yuan, *Phys. Lett. B* **682**, 207 (2009), [arXiv:0906.1454 \[hep-ph\]](#).
- [20] B.-W. Xiao, F. Yuan, and J. Zhou, *Nucl. Phys. B* **921**, 104 (2017), [arXiv:1703.06163 \[hep-ph\]](#).
- [21] P. Caucal, E. Iancu, A. H. Mueller, and F. Yuan, *Phys. Rev. Lett.* **134**, 061903 (2025), [arXiv:2408.03129 \[hep-ph\]](#).
- [22] X.-B. Tong, B.-W. Xiao, and Y.-Y. Zhang, *Phys. Rev. Lett.* **130**, 151902 (2023), [arXiv:2211.01647 \[hep-ph\]](#).
- [23] Y. Hatta, B.-W. Xiao, and F. Yuan, *Phys. Rev. D* **106**, 094015 (2022), [arXiv:2205.08060 \[hep-ph\]](#).
- [24] S. Hauksson, E. Iancu, A. H. Mueller, D. N. Triantafyllopoulos, and S. Y. Wei, *JHEP* **06**, 180 (2024), [arXiv:2402.14748 \[hep-ph\]](#).
- [25] F. Dominguez, B.-W. Xiao, and F. Yuan, *Phys. Rev. Lett.* **106**, 022301 (2011), [arXiv:1009.2141 \[hep-ph\]](#).
- [26] F. Dominguez, C. Marquet, B.-W. Xiao, and F. Yuan, *Phys. Rev. D* **83**, 105005 (2011), [arXiv:1101.0715 \[hep-ph\]](#).
- [27] A. Metz and J. Zhou, *Phys. Rev. D* **84**, 051503 (2011), [arXiv:1105.1991 \[hep-ph\]](#).
- [28] F. Dominguez, J.-W. Qiu, B.-W. Xiao, and F. Yuan, *Phys. Rev. D* **85**, 045003 (2012), [arXiv:1109.6293 \[hep-ph\]](#).
- [29] A. Dumitru, T. Lappi, and V. Skokov, *Phys. Rev. Lett.* **115**, 252301 (2015), [arXiv:1508.04438 \[hep-ph\]](#).
- [30] P. Kotko, K. Kutak, C. Marquet, E. Petreska, S. Sapeta, and A. van Hameren, *JHEP* **09**, 106 (2015), [arXiv:1503.03421 \[hep-ph\]](#).
- [31] C. Marquet, E. Petreska, and C. Roiesnel, *JHEP* **10**, 065 (2016), [arXiv:1608.02577 \[hep-ph\]](#).
- [32] C. Marquet, C. Roiesnel, and P. Tael, *Phys. Rev. D* **97**, 014004 (2018), [arXiv:1710.05698 \[hep-ph\]](#).
- [33] A. Stasto, S.-Y. Wei, B.-W. Xiao, and F. Yuan, *Phys. Lett. B* **784**, 301 (2018), [arXiv:1805.05712 \[hep-ph\]](#).
- [34] J. L. Albacete, G. Giacalone, C. Marquet, and M. Matas, *Phys. Rev. D* **99**, 014002 (2019), [arXiv:1805.05711 \[hep-ph\]](#).
- [35] A. Dumitru, V. Skokov, and T. Ullrich, *Phys. Rev. C* **99**, 015204 (2019), [arXiv:1809.02615 \[hep-ph\]](#).
- [36] T. Altinoluk, R. Boussarie, C. Marquet, and P. Tael, *JHEP* **07**, 079 (2019), [arXiv:1810.11273 \[hep-ph\]](#).
- [37] H. Mäntysaari, N. Mueller, F. Salazar, and B. Schenke, *Phys. Rev. Lett.* **124**, 112301 (2020), [arXiv:1912.05586 \[nucl-th\]](#).
- [38] T. Altinoluk and R. Boussarie, *JHEP* **10**, 208 (2019), [arXiv:1902.07930 \[hep-ph\]](#).
- [39] R. Boussarie and Y. Mehtar-Tani, *Phys. Lett. B* **831**, 137125 (2022), [arXiv:2006.14569 \[hep-ph\]](#).
- [40] T. Altinoluk, R. Boussarie, C. Marquet, and P. Tael, *JHEP* **07**, 143 (2020), [arXiv:2001.00765 \[hep-ph\]](#).
- [41] R. Boussarie, H. Mäntysaari, F. Salazar, and B. Schenke, *JHEP* **09**, 178 (2021), [arXiv:2106.11301 \[hep-ph\]](#).
- [42] E. Iancu, A. H. Mueller, D. N. Triantafyllopoulos, and S. Y. Wei, *JHEP* **10**, 103 (2022), [arXiv:2207.06268 \[hep-ph\]](#).
- [43] S. Benić, O. Garcia-Montero, and A. Perkov, *Phys. Rev. D* **105**, 114052 (2022), [arXiv:2203.01685 \[hep-ph\]](#).
- [44] F. Deganutti, C. Royon, and S. Schlichting, *JHEP* **01**, 159 (2024), [arXiv:2311.01965 \[hep-ph\]](#).
- [45] I. Ganguli, A. van Hameren, P. Kotko, and K. Kutak, *Eur. Phys. J. C* **83**, 868 (2023), [arXiv:2306.04706 \[hep-ph\]](#).
- [46] A. van Hameren, H. Kakkad, P. Kotko, K. Kutak, and S. Sapeta, *Eur. Phys. J. C* **83**, 947 (2023), [arXiv:2306.17513 \[hep-ph\]](#).

- [47] V. Cheung, Z.-B. Kang, F. Salazar, and R. Vogt, *Phys. Rev. D* **110**, 094039 (2024), [arXiv:2409.04080 \[hep-ph\]](#).
- [48] P. Kotko, K. Kutak, S. Sapeta, A. M. Stasto, and M. Strikman, *Eur. Phys. J. C* **77**, 353 (2017), [arXiv:1702.03063 \[hep-ph\]](#).
- [49] E. Iancu, A. H. Mueller, and D. N. Triantafyllopoulos, *Phys. Rev. Lett.* **128**, 202001 (2022), [arXiv:2112.06353 \[hep-ph\]](#).
- [50] P. Caucal and E. Iancu, *Phys. Rev. D* **111**, 074008 (2025), [arXiv:2406.04238 \[hep-ph\]](#).
- [51] J.-W. Qiu, W. Vogelsang, and F. Yuan, *Phys. Rev. D* **76**, 074029 (2007), [arXiv:0706.1196 \[hep-ph\]](#).
- [52] C. J. Bomhof, P. J. Mulders, and F. Pijlman, *Eur. Phys. J. C* **47**, 147 (2006), [arXiv:hep-ph/0601171](#).
- [53] T. Altinoluk, N. Armesto, and G. Beuf, *Phys. Rev. D* **108**, 074023 (2023), [arXiv:2303.12691 \[hep-ph\]](#).
- [54] T. Altinoluk, G. Beuf, and S. Mulani, *Phys. Rev. D* **111**, 034028 (2025), [arXiv:2411.15047 \[hep-ph\]](#).
- [55] T. Altinoluk, G. Beuf, E. Blanco, and S. Mulani, (2024), [arXiv:2412.08485 \[hep-ph\]](#).
- [56] B. Z. Kopeliovich, L. I. Lapidus, and A. B. Zamolodchikov, *JETP Lett.* **33**, 595 (1981).
- [57] G. Bertsch, S. J. Brodsky, A. S. Goldhaber, and J. F. Gunion, *Phys. Rev. Lett.* **47**, 297 (1981).
- [58] A. H. Mueller, *Nucl. Phys.* **B335**, 115 (1990).
- [59] N. N. Nikolaev and B. Zakharov, *Z. Phys.* **C49**, 607 (1991).
- [60] P. Caucal and F. Salazar, (2025), [arXiv:2502.02634 \[hep-ph\]](#).
- [61] I. Kolbé, K. Roy, F. Salazar, B. Schenke, and R. Venugopalan, *JHEP* **01**, 052 (2021), [arXiv:2008.04372 \[hep-ph\]](#).
- [62] I. Balitsky, *Nucl. Phys.* **B463**, 99 (1996), [arXiv:hep-ph/9509348](#).
- [63] Y. V. Kovchegov, *Phys. Rev. D* **60**, 034008 (1999), [arXiv:hep-ph/9901281](#).
- [64] J. Jalilian-Marian, A. Kovner, A. Leonidov, and H. Weigert, *Nucl. Phys.* **B504**, 415 (1997), [arXiv:hep-ph/9701284](#).
- [65] J. Jalilian-Marian, A. Kovner, A. Leonidov, and H. Weigert, *Phys. Rev. D* **59**, 014014 (1998), [arXiv:hep-ph/9706377 \[hep-ph\]](#).
- [66] A. Kovner, J. G. Milhano, and H. Weigert, *Phys. Rev. D* **62**, 114005 (2000), [arXiv:hep-ph/0004014](#).
- [67] H. Weigert, *Nucl. Phys.* **A703**, 823 (2002), [arXiv:hep-ph/0004044](#).
- [68] E. Iancu, A. Leonidov, and L. D. McLerran, *Nucl. Phys.* **A692**, 583 (2001), [arXiv:hep-ph/0011241](#).
- [69] E. Iancu, A. Leonidov, and L. D. McLerran, *Phys. Lett.* **B510**, 133 (2001), [arXiv:hep-ph/0102009](#).
- [70] E. Ferreiro, E. Iancu, A. Leonidov, and L. McLerran, *Nucl. Phys.* **A703**, 489 (2002), [arXiv:hep-ph/0109115](#).
- [71] T. Altinoluk, J. Jalilian-Marian, and C. Marquet, *Phys. Rev. D* **110**, 094056 (2024), [arXiv:2406.08277 \[hep-ph\]](#).
- [72] S. Catani and F. Hautmann, *Nucl. Phys.* **B427**, 475 (1994), [arXiv:hep-ph/9405388 \[hep-ph\]](#).
- [73] M. Ciafaloni and D. Colferai, *JHEP* **09**, 069 (2005), [arXiv:hep-ph/0507106](#).
- [74] F. Hautmann, M. Hentschinski, and H. Jung, *Nucl. Phys.* **B865**, 54 (2012), [arXiv:1205.1759 \[hep-ph\]](#).
- [75] M. Hentschinski, A. Kusina, K. Kutak, and M. Serino, *Eur. Phys. J. C* **78**, 174 (2018), [arXiv:1711.04587 \[hep-ph\]](#).
- [76] L. D. McLerran and R. Venugopalan, *Phys. Rev. D* **49**, 3352 (1994), [arXiv:hep-ph/9311205](#).
- [77] L. D. McLerran and R. Venugopalan, *Phys. Rev. D* **49**, 2233 (1994), [arXiv:hep-ph/9309289](#).
- [78] A. H. Mueller, B.-W. Xiao, and F. Yuan, *Phys. Rev. Lett.* **110**, 082301 (2013), [arXiv:1210.5792 \[hep-ph\]](#).
- [79] A. Mueller, B.-W. Xiao, and F. Yuan, *Phys. Rev. D* **88**, 114010 (2013), [arXiv:1308.2993 \[hep-ph\]](#).
- [80] Y. Hatta, B.-W. Xiao, F. Yuan, and J. Zhou, *Phys. Rev. D* **104**, 054037 (2021), [arXiv:2106.05307 \[hep-ph\]](#).
- [81] P. Taels, T. Altinoluk, G. Beuf, and C. Marquet, *JHEP* **10**, 184 (2022), [arXiv:2204.11650 \[hep-ph\]](#).
- [82] S. Mukherjee, V. V. Skokov, A. Tarasov, and S. Tiwari, *Phys. Rev. D* **109**, 034035 (2024), [arXiv:2311.16402 \[hep-ph\]](#).
- [83] P. Caucal, F. Salazar, B. Schenke, T. Stebel, and R. Venugopalan, *Phys. Rev. Lett.* **132**, 081902 (2024), [arXiv:2308.00022 \[hep-ph\]](#).
- [84] P. Caucal and F. Salazar, *JHEP* **12**, 130 (2024), [arXiv:2405.19404 \[hep-ph\]](#).
- [85] H. Duan, A. Kovner, and M. Lublinsky, *Phys. Rev. D* **111**, 054022 (2025), [arXiv:2407.15960 \[hep-ph\]](#).
- [86] L. Zheng, E. Aschenauer, J. Lee, and B.-W. Xiao, *Phys. Rev. D* **89**, 074037 (2014), [arXiv:1403.2413 \[hep-ph\]](#).
- [87] A. van Hameren, *Comput. Phys. Commun.* **224**, 371 (2018), [arXiv:1611.00680 \[hep-ph\]](#).
- [88] K. Cassar, Z. Wang, X. Chu, and E.-C. Aschenauer, (2025), [arXiv:2503.08447 \[hep-ph\]](#).
- [89] A. Ayala, M. Hentschinski, J. Jalilian-Marian, and M. E. Tejeda-Yeomans, *Phys. Lett. B* **761**, 229 (2016), [arXiv:1604.08526 \[hep-ph\]](#).
- [90] A. Ayala, M. Hentschinski, J. Jalilian-Marian, and M. E. Tejeda-Yeomans, *Nucl. Phys. B* **920**, 232 (2017), [arXiv:1701.07143 \[hep-ph\]](#).
- [91] E. Iancu and Y. Mulian, *JHEP* **07**, 121 (2023), [arXiv:2211.04837 \[hep-ph\]](#).
- [92] P. Caucal, F. Salazar, and R. Venugopalan, *JHEP* **11**, 222 (2021), [arXiv:2108.06347 \[hep-ph\]](#).
- [93] F. Bergabo and J. Jalilian-Marian, *Phys. Rev. D* **106**, 054035 (2022), [arXiv:2207.03606 \[hep-ph\]](#).
- [94] F. Bergabo and J. Jalilian-Marian, *Phys. Rev. D* **107**, 054036 (2023), [arXiv:2301.03117 \[hep-ph\]](#).
- [95] Z.-B. Kang, E. Li, and F. Salazar, *JHEP* **03**, 027 (2024), [arXiv:2310.12102 \[hep-ph\]](#).

Supplemental material

CONTENTS

Roadmap of the Calculation	8
Amplitudes for $q\bar{q}g$ production in DIS in the CGC: general results	11
Conventions and Notations	11
Amplitudes in coordinate space	12
Amplitudes in momentum space	14
Amplitudes: extracting the leading power in K_\perp/P_\perp and Q_s/P_\perp	16
Differential cross-section for inclusive back-back quark-gluon-dijet production in DIS	20
A useful change of variable	20
Integrating over the soft antiquark transverse momentum	21
Final result for the TMD factorised cross-section	21
Differential cross-section for inclusive quark-gluon dijet in gluon-initiated proton-nucleus collisions	22

In this Supplemental Material (SM), we explicitly compute the inclusive quark+gluon dijet production differential cross-section in DIS at small x in the dipole frame within the CGC effective field theory, and in the limit where the two produced jets are back-to-back in the transverse plane. In particular, we provide proofs for Eqs. (2), and (4) in the main text, corresponding to the amplitude and differential cross-section respectively, in the case of a longitudinally polarized virtual photon. We provide analogous results in the phenomenologically more relevant case of transversely polarized virtual photons. Lastly, we provide the results for the amplitudes and differential cross-section for gluon-quark dijets in the gluon-initiated pA collisions. An important outcome of our work is to obtain explicit expressions for the small- x sea quark TMDs which can be computed in the CGC.

Roadmap of the Calculation

In this section, we briefly outline the calculation of the leading power contribution to differential cross-section for inclusive quark+gluon jets in DIS. The detailed derivations can be found in the next sections. We carry out our derivation in momentum space. We refer the reader to [24] for the leading power extraction in the diffractive case, where quark TMD factorisation for quark-gluon dijets was also found.

The coordinate space results for the amplitudes for inclusive quark+gluon+antiquark production in DIS within the CGC, for general trijet small- x kinematics can be found in [89–95]. We begin by expressing these amplitudes in momentum space. At amplitude level there are four contributions as shown in Fig. 7, their contributions can be organized as a convolution

$$\begin{aligned} \mathcal{M}_{qg(\bar{q}),\sigma\bar{\sigma},i\bar{i}}^{\lambda\bar{\lambda},a}(k_q, k_{\bar{q}}, k_g) = \int \frac{d^2\mathbf{q}_2}{(2\pi)^2} \left\{ \int \frac{d^2\mathbf{q}_1}{(2\pi)^2} \left[\mathcal{J}_{R1,\sigma\bar{\sigma}}^{\lambda\bar{\lambda}}(\mathbf{q}_1, \mathbf{q}_2) + \mathcal{J}_{\bar{R}1,\sigma\bar{\sigma}}^{\lambda\bar{\lambda}}(\mathbf{q}_1, \mathbf{q}_2) \right] \mathcal{C}_{R1,i\bar{i}}^a(\mathbf{q}_1, \mathbf{q}_2) \right. \\ \left. + \mathcal{J}_{R2,\sigma\bar{\sigma}}^{\lambda\bar{\lambda}}(\mathbf{q}_2) \mathcal{C}_{R2,i\bar{i}}^a(\mathbf{q}_2) + \mathcal{J}_{\bar{R}2,\sigma\bar{\sigma}}^{\lambda\bar{\lambda}}(\mathbf{q}_2) \mathcal{C}_{\bar{R}2,i\bar{i}}^a(\mathbf{q}_2) \right\}, \end{aligned} \quad (14)$$

where $\mathcal{J}_{X,\sigma\bar{\sigma}}^{\lambda\bar{\lambda}}$ and $\mathcal{C}_{X,i\bar{i}}^a$ are the perturbative factors and color operators corresponding to the four different diagrams. For diagrams R1 and $\bar{R}1$, in which the shockwave interacts with the three partons, there are two loop momenta due to multiple scattering \mathbf{q}_1 and \mathbf{q}_2 which we define such that they correspond to the transverse momenta transferred from the shockwave to the quark and antiquark respectively (the momentum transfer to the gluon follows from momentum conservation $\mathbf{k}_g + \mathbf{k}_q + \mathbf{k}_{\bar{q}} - \mathbf{q}_1 - \mathbf{q}_2$). For diagrams R2 and $\bar{R}2$ there is only one loop momenta which we choose to be that of the momentum transfer from the shockwave to the antiquark (the momentum transfer to the quark follows from momentum conservation $\mathbf{k}_g + \mathbf{k}_q + \mathbf{k}_{\bar{q}} - \mathbf{q}_2$).

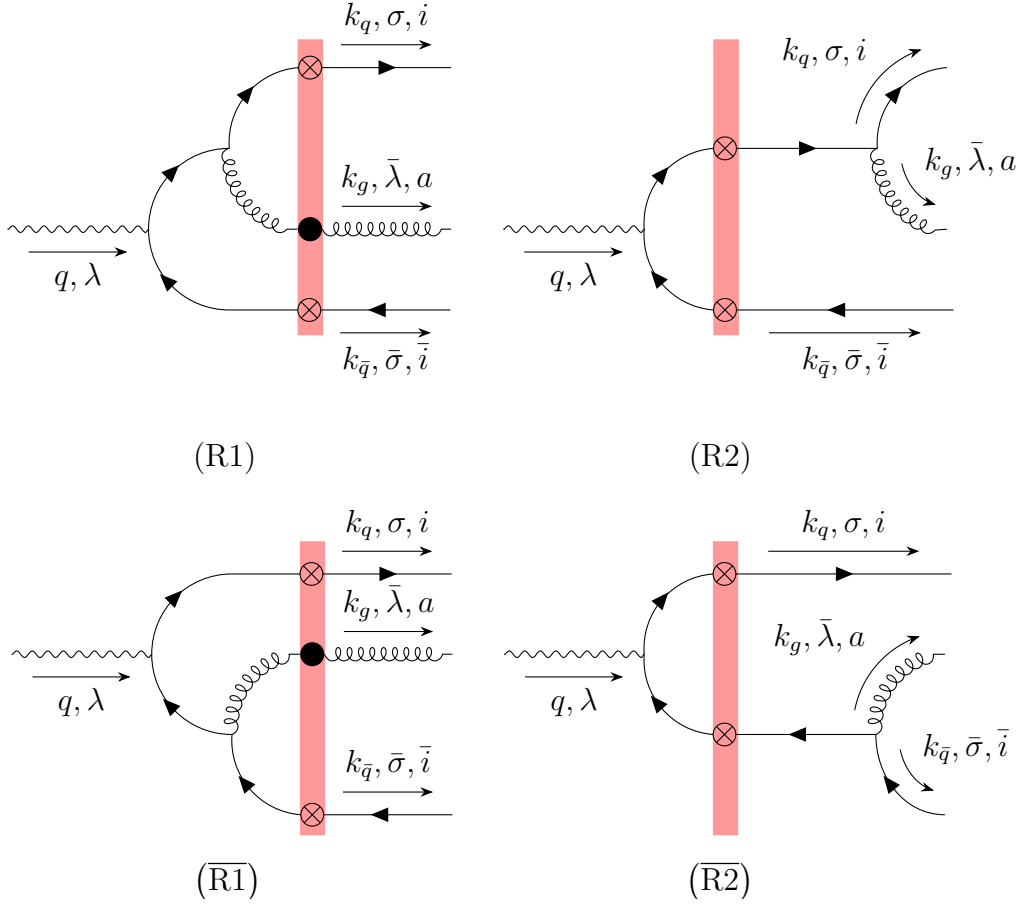


Figure 7. The four diagrams contributing to $q\bar{q}g$ production in DIS within the CGC. Top diagrams correspond to gluon emission from quark. Bottom diagrams to gluon emission from antiquark. The crossed dot denotes the effective quark CGC vertex, and the bullet (full circle) denotes the effective CGC gluon vertex. The helicity and color of the quark (antiquark) are denoted as σ ($\bar{\sigma}$) and i (\bar{i}) respectively, and the polarizations of the photon and gluon as λ and $\bar{\lambda}$ respectively. The color index of the gluon is denoted as a .

Next, we isolate the leading power contribution when the quark and gluon are back-to-back:

$$K_{\perp}, Q_s \ll P_{\perp}, \quad (15)$$

where $\mathbf{K} = \mathbf{k}_q + \mathbf{k}_{\bar{q}}$ is the transverse momentum imbalance, and $\mathbf{P} = (z_g \mathbf{k}_q - z_{\bar{q}} \mathbf{k}_{\bar{q}})/(z_q + z_g)$ is the transverse relative momentum.

We perform the leading power expansion at the amplitude level and in momentum space, which has the advantage of tremendously simplifying the intermediate expression for the sum of all relevant amplitudes and giving a transparent hierarchy of the scales. The typical momentum transfer imparted by the shockwave to the partons is controlled by the saturation scale Q_s ; thus, the condition $Q_s \ll P_{\perp}$ implies that $|\mathbf{q}_1|, |\mathbf{q}_2| \ll P_{\perp}$. To leading power accuracy the perturbative factors for R1 and $\overline{\text{R1}}$ become independent of \mathbf{q}_1 , and the perturbative factor for $\overline{\text{R2}}$ becomes independent of \mathbf{q}_2 . Then we can express the total amplitude as

$$\begin{aligned} \mathcal{M}_{qg(\bar{q}),\sigma\bar{\sigma},i\bar{i}}^{\lambda\bar{\lambda},a}(k_q, k_{\bar{q}}, k_g) = & \int \frac{d^2 \mathbf{q}_2}{(2\pi)^2} \left\{ \left[\mathcal{J}_{\text{R1},\sigma\bar{\sigma}}^{\lambda\bar{\lambda}}(\mathbf{q}_2) + \mathcal{J}_{\overline{\text{R1}},\sigma\bar{\sigma}}^{\lambda\bar{\lambda}}(\mathbf{q}_2) \right] \int \frac{d^2 \mathbf{q}_1}{(2\pi)^2} C_{\text{R1},i\bar{i}}^a(\mathbf{q}_1, \mathbf{q}_2) \right. \\ & \left. + \mathcal{J}_{\text{R2},\sigma\bar{\sigma}}^{\lambda\bar{\lambda}}(\mathbf{q}_2) C_{\text{R2},i\bar{i}}^a(\mathbf{q}_2) + \mathcal{J}_{\overline{\text{R2}},\sigma\bar{\sigma}}^{\lambda\bar{\lambda}} C_{\overline{\text{R2}},i\bar{i}}^a(\mathbf{q}_2) \right\}. \end{aligned} \quad (16)$$

Due to unitarity of the Wilson lines we have

$$\int \frac{d^2 \mathbf{q}_1}{(2\pi)^2} C_{R1, i\bar{i}}^a(\mathbf{q}_1, \mathbf{q}_2) = C_{R2, i\bar{i}}^a(\mathbf{q}_2), \quad (17)$$

$$\int \frac{d^2 \mathbf{q}_2}{(2\pi)^2} C_{R2, i\bar{i}}^a(\mathbf{q}_2) = 0. \quad (18)$$

Thus at leading power the amplitude can be written as

$$\mathcal{M}_{qg(\bar{q}), \sigma\bar{\sigma}, i\bar{i}}^{\lambda\bar{\lambda}, a}(k_q, k_{\bar{q}}, k_g) = \int \frac{d^2 \mathbf{q}_2}{(2\pi)^2} \left[\mathcal{J}_{q, \sigma\bar{\sigma}}^{\lambda\bar{\lambda}}(\mathbf{q}_2) + \mathcal{J}_{\bar{q}, \sigma\bar{\sigma}}^{\lambda\bar{\lambda}}(\mathbf{q}_2) \right] C_{R2, i\bar{i}}^a(\mathbf{q}_2), \quad (19)$$

where we summed the introduced the perturbative factors

$$\mathcal{J}_{q, \sigma\bar{\sigma}}^{\lambda\bar{\lambda}}(\mathbf{q}_2) = \mathcal{J}_{R1, \sigma\bar{\sigma}}^{\lambda=, \bar{\lambda}}(\mathbf{q}_2) + \mathcal{J}_{R2, \sigma\bar{\sigma}}^{\lambda=, \bar{\lambda}}(\mathbf{q}_2), \quad (20)$$

$$\mathcal{J}_{\bar{q}, \sigma\bar{\sigma}}^{\lambda\bar{\lambda}}(\mathbf{q}_2) = \mathcal{J}_{R1, \sigma\bar{\sigma}}^{\lambda=, \bar{\lambda}}(\mathbf{q}_2). \quad (21)$$

We then recognize that these two perturbative factors posses the light-cone denominator

$$\frac{1}{\left[z_{\bar{q}} \left(Q^2 + \frac{\mathbf{P}^2}{z_q z_g} \right) + (\mathbf{q}_2 - \mathbf{k}_{\bar{q}})^2 \right]}. \quad (22)$$

Thus we see that the leading power contribution in the back-to-back limit demands the unobserved antiquark to have small momentum fraction $z_{\bar{q}} \lesssim \max(K^2, Q_s^2)/P_{\perp}^2 \ll 1$, and the measured quark and gluon jets carry the total longitudinal momentum of the virtual photon $z_q + z_g \approx 1$. This is analogous to the dominance of the aligned jet configuration in SIDIS at high Q^2 . Expanding the perturbative factors for small values of $z_{\bar{q}} \sim K_{\perp}^2/P_{\perp}^2$, and performing the shift of variables $\ell = \mathbf{q}_2 - \mathbf{k}_{\bar{q}}$, we find

$$\begin{aligned} \mathcal{M}_{qg(\bar{q}), \sigma\bar{\sigma}, i\bar{i}}^{\lambda=\pm 1, \bar{\lambda}, a} &= -8eefg\sqrt{z_q z_{\bar{q}}} q^+ \delta^{\sigma, -\bar{\sigma}} \int \frac{d^2 \ell}{(2\pi)^2} \frac{1}{\ell^2 + z_{\bar{q}}(Q^2 + M_{qg}^2)} C_{1, i\bar{i}}^a(\mathbf{K} - \ell, \ell + \mathbf{k}_{\bar{q}}) \\ &\times \frac{1}{z_q z_g} \left\{ \delta^{\sigma, -\lambda} \left[\delta^{\lambda\bar{\lambda}} + z_q \delta^{\lambda, -\bar{\lambda}} \right] \frac{(\mathbf{P} \cdot \boldsymbol{\epsilon}^{\bar{\lambda}*})(\ell \cdot \boldsymbol{\epsilon}^{\lambda})}{M_{qg}^2} + \delta^{\sigma, \bar{\lambda}} \left[z_g \delta^{\lambda, \bar{\lambda}} - z_q \delta^{\lambda, -\bar{\lambda}} \right] \frac{(\mathbf{P} \cdot \boldsymbol{\epsilon}^{\lambda})(\ell \cdot \boldsymbol{\epsilon}^{\bar{\lambda}*})}{M_{qg}^2 + Q^2} \right\}, \end{aligned} \quad (23)$$

$$\mathcal{M}_{qg(\bar{q}), \sigma\bar{\sigma}, i\bar{i}}^{\lambda=0, \bar{\lambda}, a} = 8eefg\sqrt{z_q z_{\bar{q}}} q^+ \delta^{\sigma, -\bar{\sigma}} \delta^{\bar{\lambda}\sigma} \frac{Q}{M_{qg}^2 + Q^2} \int \frac{d^2 \ell}{(2\pi)^2} \frac{\ell \cdot \boldsymbol{\epsilon}^{\bar{\lambda}*}}{\ell^2 + z_{\bar{q}}(Q^2 + M_{qg}^2)} C_{1, i\bar{i}}^a(\mathbf{K} - \ell, \ell + \mathbf{k}_{\bar{q}}), \quad (24)$$

where we defined

$$C_{1, i\bar{i}}^a(\mathbf{q}_1, \mathbf{q}_2) = \int d^2 \mathbf{x} d^2 \mathbf{y} e^{-i\mathbf{q}_1 \cdot \mathbf{x} - i\mathbf{q}_2 \cdot \mathbf{y}} \left[t^a V(\mathbf{x}) V^\dagger(\mathbf{y}) - t^a \right]_{i\bar{i}}. \quad (25)$$

For transversely polarized photons, both the emission from quark and antiquark contribute to the amplitude, while for the longitudinally polarized photons only the gluon emission from the antiquark before the shockwave survives at leading power.

Lastly, we compute the cross-section by squaring this amplitude and integrating over the phase space of the antiquark ($z_{\bar{q}}, \mathbf{k}_{\bar{q}}$)

$$\frac{d\sigma^{\gamma^* A \rightarrow qg+X}}{d^2 \mathbf{P} d^2 \mathbf{K} dz_g dz_q} = H^\lambda(z_q, Q^2, \mathbf{P}) \times xq^{(1)}(x, \mathbf{K}), \quad (26)$$

where the hard factors for longitudinally and transversely polarized photons are

$$H^{\lambda=0}(z_q, Q^2, \mathbf{P}) = \alpha_s C_F \alpha_{em} e_f^2 \delta(1 - z_q - z_g) \frac{8Q^2 z_q^3 z_g^2}{[z_q z_g Q^2 + \mathbf{P}^2]^3}, \quad (27)$$

$$H^{\lambda=\pm 1}(z_q, Q^2, \mathbf{P}) = \alpha_s C_F \alpha_{em} e_f^2 \delta(1 - z_q - z_g) \frac{2z_q \left\{ [\mathbf{P}^2 + z_q z_g Q^2]^2 + z_g^2 (\mathbf{P})^4 + z_q^4 z_g^2 Q^2 \right\}}{\mathbf{P}^2 [z_q z_g Q^2 + \mathbf{P}^2]^3}, \quad (28)$$

respectively. The small- x sea-quark TMD is given by

$$xq^{(1)}(x, \mathbf{K}) = \frac{N_c}{4\pi^4} \int d^2b d^2q \left\langle \mathcal{D}_F^{(1)}(\mathbf{b}, \mathbf{q}) \right\rangle_x \left\{ 1 - \frac{\mathbf{K} \cdot (\mathbf{K} - \mathbf{q})}{K_\perp^2 - (\mathbf{K} - \mathbf{q})^2} \ln \left(\frac{K_\perp^2}{(\mathbf{K} - \mathbf{q})^2} \right) \right\}, \quad (29)$$

where we introduced the Fourier transform of the dipole correlator

$$\mathcal{D}_F^{(1)}(\mathbf{b}, \mathbf{q}) \equiv \int d^2r \frac{e^{-i\mathbf{q} \cdot \mathbf{r}}}{(2\pi)^2} \left(\frac{1}{N_c} \text{Tr} \left[V_{\mathbf{b}+\mathbf{r}/2} V_{\mathbf{b}-\mathbf{r}/2}^\dagger \right] \right). \quad (30)$$

Amplitudes for $q\bar{q}g$ production in DIS in the CGC: general results

Conventions and Notations

We work with lightcone coordinates

$$v^\pm = \frac{1}{\sqrt{2}}(v^0 \pm v^3), \quad (31)$$

with the transverse momenta components the same as Minkowski space. Four-vectors will be defined as $v^\mu = (v^+, v^-, \mathbf{v})$ where $\mathbf{v} = (v^1, v^2)$ denotes two-dimensional transverse components. Throughout this SM, we will contract the two-dimensional vectors with Euclidean metric, such that the scalar product of four vectors reads

$$v^\mu w_\mu = v^+ w^- + v^- w^+ - \mathbf{v} \cdot \mathbf{w} = v^\mu w_\mu = v^+ w^- + v^- w^+ - \mathbf{v}^j \mathbf{w}^j. \quad (32)$$

We work in the dipole frame where a nucleon from the nucleus target has four-momentum

$$P_N^\mu = (0, P_N^-, \mathbf{0}), \quad (33)$$

where we neglected the mass m_N of the nucleon $m_N \ll P_N^-$, and the virtual photon has four-momentum

$$q^\mu = \left(q^+, -\frac{Q^2}{2q^+}, \mathbf{0} \right). \quad (34)$$

The final state quark, antiquark, and gluon have momenta

$$k_q^\mu = \left(z_q q^+, \frac{(\mathbf{k}_q)^2}{2z_q q^+}, \mathbf{k}_q \right), \quad k_{\bar{q}}^\mu = \left(z_{\bar{q}} q^+, \frac{(\mathbf{k}_{\bar{q}})^2}{2z_{\bar{q}} q^+}, \mathbf{k}_{\bar{q}} \right), \quad k_g^\mu = \left(z_g q^+, \frac{(\mathbf{k}_g)^2}{2z_g q^+}, \mathbf{k}_g \right), \quad (35)$$

respectively. Let us define the relative momentum and momentum imbalance of the quark+gluon system

$$\mathbf{P} = \frac{z_g \mathbf{k}_q - z_q \mathbf{k}_g}{z_q + z_g}, \quad (36)$$

$$\mathbf{K} = \mathbf{k}_q + \mathbf{k}_g, \quad (37)$$

respectively.

We will denote the helicity and color of the quark (antiquark) as σ ($\bar{\sigma}$) and i (\bar{i}) respectively, and the polarizations of the photon and gluon as λ and $\bar{\lambda}$ respectively. The color index of the gluon is denoted as a . The strong coupling, electromagnetic coupling and fractional quark charge are denoted as g , e and e_f respectively.

The large- x partons in the fast moving nucleus generate a current $J^{\mu,c}(z) = \delta^{\mu-} \rho^c(z^+, z)$. In the light-cone gauge $A_{\text{cl}}^- = 0$, the classical background field sourced by this current is given by

$$A_{\text{cl}}^{\mu,c}(z) = \delta^{\mu-} A_{\text{cl}}^{-,c}(z^+, z) \quad (38)$$

where $A^{-,c}$ satisfies the Poisson equation:

$$\nabla_\perp^2 A_{\text{cl}}^{-,c}(z^+, z) = -\rho^c(z^+, z). \quad (39)$$

The effective vertices for the interaction of the quark, antiquark, and gluon with the background field are

$$\mathcal{T}_{\sigma\bar{\sigma},ij}^q(l,l') = (2\pi)\delta(l^+ - l'^+)\gamma^+ \int d^2\mathbf{x} e^{-i(\ell-\ell')\cdot\mathbf{x}} V_{ij}(\mathbf{x}), \quad (40)$$

$$\mathcal{T}_{\sigma\bar{\sigma},ij}^{\bar{q}}(l,l') = -(2\pi)\delta(l^+ - l'^+)\gamma^+ \int d^2\mathbf{x} e^{-i(\ell-\ell')\cdot\mathbf{x}} V_{ij}^\dagger(\mathbf{x}), \quad (41)$$

$$\mathcal{T}_{\mu\nu,ab}^g(l,l') = -(2\pi)\delta(l^+ - l'^+)(2l^+) g_{\mu\nu} \int d^2\mathbf{z} e^{-i(\ell-\ell')\cdot\mathbf{z}} U_{ab}(\mathbf{z}). \quad (42)$$

respectively, and the light-like Wilson lines in fundamental and adjoint representations read:

$$V_{ij}(\mathbf{x}) = \mathcal{P} \exp \left(ig \int_{-\infty}^{\infty} dz^+ A_{\text{cl}}^{-,a}(z^+, \mathbf{x}) t_{ij}^a \right), \quad (43)$$

$$U_{ab}(\mathbf{x}) = \mathcal{P} \exp \left(ig \int_{-\infty}^{\infty} dz^+ A_{\text{cl}}^{-,c}(z^+, \mathbf{x}) T_{ab}^c \right), \quad (44)$$

with t^a and T^c are generators of SU(3) in the fundamental and adjoint representation, respectively.

Let us define the two-dimensional transverse vector:

$$\epsilon_{\perp}^{\lambda=\pm 1} = \frac{1}{\sqrt{2}}(1, \lambda i). \quad (45)$$

The explicit expression for polarization vectors of the virtual photon reads

$$\epsilon^\mu(q, \lambda = \pm 1) = (0, 0, \epsilon_{\perp}^{\lambda}), \quad (46)$$

for the two transverse polarizations $\lambda = \pm 1$, and

$$\epsilon^\mu(q, \lambda = 0) = \left(0, \frac{Q}{q^+}, \mathbf{0} \right), \quad (47)$$

for the longitudinal polarization, which we denote as $\lambda = 0$. For the final state gluon the polarization vectors read:

$$\epsilon^{\mu*}(k_g, \bar{\lambda} = \pm 1) = \left(0, \frac{\epsilon_{\perp}^{\bar{\lambda}*} \cdot \mathbf{k}_g}{k_g^+}, \epsilon_{\perp}^{\bar{\lambda}*} \right). \quad (48)$$

Amplitudes in coordinate space

The amplitudes for $q\bar{q}g$ production in DIS in the CGC were computed by several groups [89–94] (see also [95] including quark mass effects). We summarize here the results for the amplitudes (shown in Fig. 7) in coordinate space, considering first the diagram where the gluon is emitted by the quark before the shockwave, labeled R1 and then the diagram where the gluon is emitted by the quark after the shockwave and labeled R2. As discussed in the following subsection, the other two amplitudes associated with gluon emissions by the antiquark, labeled $\bar{R}1$ and $\bar{R}2$, can be obtained from R1 and R2 from quark-antiquark exchange.

Gluon emission from the quark before the shockwave. The amplitude R1 reads, for general $q\bar{q}g$ kinematics at small x ,

$$\begin{aligned} \mathcal{M}_{\text{R1},\sigma\bar{\sigma},i\bar{i}}^{\lambda\bar{\lambda},a}(k_q, k_{\bar{q}}, k_g) &= \frac{eef}{2\pi} \int d^2\mathbf{x} d^2\mathbf{y} d^2\mathbf{z} \mathcal{C}_{\text{R1},i\bar{i}}^a(\mathbf{x}, \mathbf{y}, \mathbf{z}) e^{-i\mathbf{k}_q \cdot \mathbf{x}} e^{-i\mathbf{k}_{\bar{q}} \cdot \mathbf{y}} e^{-i\mathbf{k}_g \cdot \mathbf{z}} \\ &\times \bar{u}_{\sigma}(k_q) \mathcal{N}_{\text{R1}}^{\lambda\bar{\lambda}}(k_q, k_{\bar{q}}, k_g; \mathbf{x}, \mathbf{y}, \mathbf{z}) v_{\bar{\sigma}}(k_{\bar{q}}), \end{aligned} \quad (49)$$

where the color operator:

$$\begin{aligned} \mathcal{C}_{\text{R1},i\bar{i}}^a(\mathbf{x}, \mathbf{y}, \mathbf{z}) &= [V(\mathbf{x}) t_b V^\dagger(\mathbf{y}) U^{ab}(\mathbf{z}) - t^a]_{i\bar{i}} \\ &= [V(\mathbf{x}) V^\dagger(\mathbf{z}) t^a V(\mathbf{z}) V^\dagger(\mathbf{y}) - t^a]_{i\bar{i}}, \end{aligned} \quad (50)$$

and the perturbative factor reads

$$\mathcal{N}_{R1}^{\lambda\bar{\lambda}}(k_q, k_{\bar{q}}, k_g; \mathbf{x}, \mathbf{y}, \mathbf{z}) = \frac{g}{2\pi} \int \frac{d^2\mathbf{l}_1}{(2\pi)^2} \frac{d^2\mathbf{l}_2}{(2\pi)^2} e^{i\mathbf{l}_1 \cdot (\mathbf{x} - \mathbf{y})} e^{i\mathbf{l}_2 \cdot (\mathbf{z} - \mathbf{x})} \times \left[I_{R1,reg} \mathcal{T}_{R1,reg}^{\lambda\bar{\lambda}}(l_1, l_2) + I_{R1,inst} \mathcal{T}_{R1,inst}^{\lambda\bar{\lambda}}(l_1, l_2) \right] \Big|_{\substack{l_1^+ = q^+ - q^+ z_{\bar{q}}, \\ l_2^+ = q^+ z_g}}, \quad (51)$$

with light-cone energy denominators

$$I_{R1,reg} = \frac{(2\pi)^2}{2q^+ z_g z_{\bar{q}}} \frac{1}{[Q^2 z_{\bar{q}} (1 - z_{\bar{q}}) + l_1^2] \left[Q^2 + \frac{l_1^2}{z_{\bar{q}}} + \frac{(l_2 - l_1)^2}{z_q} + \frac{l_2^2}{z_g} \right]}, \quad (52)$$

$$I_{R1,inst} = -\frac{(2\pi)^2}{2q^+ z_q z_{\bar{q}} z_g} \frac{1}{\left[Q^2 + \frac{l_1^2}{z_{\bar{q}}} + \frac{(l_2 - l_1)^2}{z_q} + \frac{l_2^2}{z_g} \right]}. \quad (53)$$

For the longitudinally polarized case, the Lorentz-Dirac structure reads

$$\mathcal{T}_{R1,reg}^{\lambda=0,\bar{\lambda}}(l_1, l_2) = -8Qq^+ z_q z_{\bar{q}} (1 - z_{\bar{q}}) \epsilon^{\bar{\lambda}*n} \left\{ \left(\mathbf{l}_2 - \frac{z_g}{1 - z_{\bar{q}}} \mathbf{l}_1 \right)^m \left[\left(1 + \frac{z_g}{2z_q} \right) \delta^{mn} - \frac{z_g}{2z_q} \omega^{mn} \right] \right\} \gamma^+, \quad (54)$$

while, for the transversely polarized photon case, it is given by

$$\mathcal{T}_{R1,reg}^{\lambda=\pm 1,\bar{\lambda}}(l_1, l_2) = -4q^+ z_q \epsilon^{\bar{\lambda}*n} \epsilon^{\lambda,k} \left\{ \left(\mathbf{l}_2 - \frac{z_g}{1 - z_{\bar{q}}} \mathbf{l}_1 \right)^m \left[\left(1 + \frac{z_g}{2z_q} \right) \delta^{mn} - \frac{z_g}{2z_q} \omega^{mn} \right] \right\} \times (\mathbf{l}_1)^j [\delta^{kj} (1 - 2z_{\bar{q}}) - \omega^{kj}] \gamma^+, \quad (55)$$

$$\mathcal{T}_{R1,inst}^{\lambda=\pm 1,\bar{\lambda}}(l_1, l_2) = 2q^+ \frac{z_g z_q z_{\bar{q}}}{1 - z_{\bar{q}}} \epsilon^{\bar{\lambda}*n} \epsilon^{\lambda,k} \gamma^n \gamma^k \gamma^+. \quad (56)$$

We introduced the commutator of transverse gamma matrices

$$\omega^{kj} = \frac{1}{2} [\gamma^k, \gamma^j], \quad (57)$$

so that we have $\gamma^k \gamma^j = -\delta^{kj} + \omega^{kj}$.

Gluon emission from the quark after the shockwave. Likewise, the amplitude associated with diagram R2 reads

$$\mathcal{M}_{R2,\sigma\bar{\sigma},i\bar{i}}^{\lambda\bar{\lambda},a}(k_q, k_{\bar{q}}, k_g) = \frac{e e_f}{2\pi} \int d^2\mathbf{x} d^2\mathbf{y} e^{-i(\mathbf{k}_q + \mathbf{k}_g) \cdot \mathbf{x}} e^{-i\mathbf{k}_{\bar{q}} \cdot \mathbf{y}} C_{R2,i\bar{i}}^a(\mathbf{x}, \mathbf{y}) \times \bar{u}_\sigma(k_q) \mathcal{N}_{R2}^{\lambda\bar{\lambda}}(k_q, k_{\bar{q}}, k_g; \mathbf{x}, \mathbf{y}) v_{\bar{\sigma}}(k_{\bar{q}}), \quad (58)$$

where the color operator:

$$C_{R2,i\bar{i}}^a(\mathbf{x}, \mathbf{y}) = [t^a V(\mathbf{x}) V^\dagger(\mathbf{y}) - t^a]_{i\bar{i}}, \quad (59)$$

and the perturbative factor reads

$$\mathcal{N}_{R2}^{\lambda\bar{\lambda}}(k_q, k_{\bar{q}}, k_g; \mathbf{x}, \mathbf{y}) = -g \int \frac{d^2\ell}{2\pi} \frac{e^{i\ell \cdot (\mathbf{x} - \mathbf{y})}}{(1 - z_{\bar{q}}) z_{\bar{q}} Q^2 + \ell^2} \mathcal{T}_{R2}^{\lambda\bar{\lambda}}(l) \Big|_{l^+ = q^+ - q^+ z_{\bar{q}}}. \quad (60)$$

The explicit expressions for the Lorentz-Dirac structures are:

$$\mathcal{T}_{R2}^{\lambda=0,\bar{\lambda}}(l) = -\frac{2Q(1 - z_{\bar{q}}) z_{\bar{q}} \epsilon^{\bar{\lambda}*n} \left\{ 2 \left(\mathbf{k}_g - \frac{z_g}{z_q} \mathbf{p}_{1\perp} \right)^m \left[\delta^{mn} \left(1 + \frac{z_g}{2z_q} \right) - \frac{z_g}{2z_q} \omega^{mn} \right] \right\} \gamma^+}{\left(\mathbf{k}_g - \frac{z_g}{z_q} \mathbf{k}_q \right)^2}, \quad (61)$$

for longitudinally polarized photons, and

$$\mathcal{T}_{R2}^{\lambda=\pm 1,\bar{\lambda}}(l) = \frac{\epsilon^{\bar{\lambda}*n} \epsilon^{\lambda,k} \left\{ 2 \left(\mathbf{k}_g - \frac{z_g}{z_q} \mathbf{k}_q \right)^m \left[\delta^{mn} \left(1 + \frac{z_g}{2z_q} \right) - \frac{z_g}{2z_q} \omega^{mn} \right] \right\}}{\left(\mathbf{k}_g - \frac{z_g}{z_q} \mathbf{k}_q \right)^2} \times (\ell)^j [\delta^{kj} (2z_{\bar{q}} - 1) + \omega^{kj}] \gamma^+, \quad (62)$$

for transversely polarized photons.

Amplitudes in momentum space

In order to perform the simplification needed for the calculation of inclusive quark+gluon dijet production with a soft antiquark integrated out, it is more convenient to express the expansion in momentum space. Hence, in this section we present the amplitudes in the momentum space representation.

Gluon emission from the quark before the shockwave. Let us perform a change of variables such that the momenta transfer to the quark and antiquark are \mathbf{q}_1 and \mathbf{q}_2 respectively:

$$\mathbf{q}_1 = \mathbf{l}_2 - \mathbf{l}_1 + \mathbf{k}_q, \quad (63)$$

$$\mathbf{q}_2 = \mathbf{l}_1 + \mathbf{k}_{\bar{q}}, \quad (64)$$

equivalently:

$$\mathbf{l}_1 = \mathbf{q}_2 - \mathbf{k}_{\bar{q}}, \quad (65)$$

$$\mathbf{l}_2 = \mathbf{q}_1 + \mathbf{q}_2 - \mathbf{k}_q - \mathbf{k}_{\bar{q}}. \quad (66)$$

These choices of momenta \mathbf{q}_1 and \mathbf{q}_2 will be more convenient when carrying out the expansion. The typical magnitudes of these momenta are of the order of the saturation scale $|\mathbf{q}_1|, |\mathbf{q}_2| \sim Q_s$. Note that this is not the case for \mathbf{l}_1 and \mathbf{l}_2 .

We can write the amplitude for gluon emission before the shock wave as:

$$\mathcal{M}_{\text{R1}, \sigma\bar{\sigma}, i\bar{i}}^{\lambda\bar{\lambda}, a}(\mathbf{k}_q, \mathbf{k}_{\bar{q}}, \mathbf{k}_g) = \int \frac{d^2\mathbf{q}_1}{(2\pi)^2} \int \frac{d^2\mathbf{q}_2}{(2\pi)^2} \mathcal{C}_{\text{R1}, i\bar{i}}^a(\mathbf{q}_1, \mathbf{q}_2) \mathcal{J}_{\text{R1}, \sigma\bar{\sigma}}^{\lambda\bar{\lambda}}(\mathbf{q}_1, \mathbf{q}_2), \quad (67)$$

where the color factor is

$$\begin{aligned} \mathcal{C}_{\text{R1}, i\bar{i}}^a(\mathbf{q}_1, \mathbf{q}_2) &= \int d^2\mathbf{x} d^2\mathbf{y} d^2\mathbf{z} e^{-i\mathbf{q}_1 \cdot \mathbf{x}} e^{-i\mathbf{q}_2 \cdot \mathbf{y}} e^{-i(\mathbf{k}_q + \mathbf{k}_{\bar{q}} + \mathbf{k}_g - \mathbf{q}_1 - \mathbf{q}_2) \cdot \mathbf{z}} \\ &\times [V(\mathbf{x}) V^\dagger(\mathbf{z}) t^a V(\mathbf{z}) V^\dagger(\mathbf{y}) - t^a]_{i\bar{i}}. \end{aligned} \quad (68)$$

The perturbative factor for longitudinally polarized photons is

$$\begin{aligned} \mathcal{J}_{\text{R1}, \sigma\bar{\sigma}}^{\lambda=0, \bar{\lambda}}(\mathbf{q}_1, \mathbf{q}_2) &= \\ &= -\frac{ee_{fg}}{z_g} \frac{4Qz_{\bar{q}}(1-z_{\bar{q}}) \epsilon^{\bar{\lambda}*n} \bar{u}_\sigma(k_q) \left\{ \left(\mathbf{q}_1 - \mathbf{k}_q + \frac{z_q}{1-z_{\bar{q}}}(\mathbf{q}_2 - \mathbf{k}_{\bar{q}}) \right)^m \left[\left(1 + \frac{z_g}{2z_q} \right) \delta^{mn} - \frac{z_g}{2z_q} \omega^{mn} \right] \right\} \gamma^+ v_{\bar{\sigma}}(k_{\bar{q}})}{[Q^2 z_{\bar{q}}(1-z_{\bar{q}}) + (\mathbf{q}_2 - \mathbf{k}_{\bar{q}})^2] \left[Q^2 + \frac{(\mathbf{q}_1 - \mathbf{k}_q)^2}{z_q} + \frac{(\mathbf{q}_1 + \mathbf{q}_2 - \mathbf{k}_q - \mathbf{k}_{\bar{q}})^2}{z_g} + \frac{(\mathbf{q}_2 - \mathbf{k}_{\bar{q}})^2}{z_{\bar{q}}} \right]}, \end{aligned} \quad (69)$$

and for transversely polarized photons, it is

$$\begin{aligned} \mathcal{J}_{\text{R1}, \sigma\bar{\sigma}}^{\lambda=\pm 1, \bar{\lambda}}(\mathbf{q}_1, \mathbf{q}_2) &= -\frac{ee_{fg} \epsilon^{\bar{\lambda}*n} \epsilon^{\lambda, k}}{\left[Q^2 + \frac{(\mathbf{q}_1 - \mathbf{k}_q)^2}{z_q} + \frac{(\mathbf{q}_1 + \mathbf{q}_2 - \mathbf{k}_q - \mathbf{k}_{\bar{q}})^2}{z_g} + \frac{(\mathbf{q}_2 - \mathbf{k}_{\bar{q}})^2}{z_{\bar{q}}} \right]} \\ &\times \bar{u}_\sigma(k_q) \left[\frac{2 \left\{ \left(\mathbf{q}_1 - \mathbf{k}_q + \frac{z_q}{1-z_{\bar{q}}}(\mathbf{q}_2 - \mathbf{k}_{\bar{q}}) \right)^m \left[\left(1 + \frac{z_g}{2z_q} \right) \delta^{mn} - \frac{z_g}{2z_q} \omega^{mn} \right] \right\}}{z_g [Q^2 z_{\bar{q}}(1-z_{\bar{q}}) + (\mathbf{q}_2 - \mathbf{k}_{\bar{q}})^2]} \right. \\ &\times \left. \left\{ (\mathbf{q}_2 - \mathbf{k}_{\bar{q}})^j [\delta^{kj}(1-2z_{\bar{q}}) - \omega^{kj}] \right\} + \frac{\gamma^n \gamma^k}{(1-z_{\bar{q}})} \right] \gamma^+ v_{\bar{\sigma}}(k_{\bar{q}}). \end{aligned} \quad (70)$$

Gluon emission from the quark after the shockwave. Here only the quark and antiquark interact with the shockwave, thus there is only one loop momentum (due to multiple scattering), which we choose to be \mathbf{q}_2 (the momentum transfer to the anti-quark).

Let us perform the change of variables:

$$\mathbf{q}_2 = \boldsymbol{\ell} + \mathbf{k}_{\bar{q}}, \quad (71)$$

then

$$\mathcal{M}_{\text{R2},\sigma\bar{\sigma},i\bar{i}}^{\lambda\bar{\lambda},a}(k_q, k_{\bar{q}}, k_g) = \int \frac{d^2\mathbf{q}_2}{(2\pi)^2} C_{\text{R2},i\bar{i}}^a(\mathbf{q}_2) \mathcal{J}_{\text{R2},\sigma\bar{\sigma}}^{\lambda\bar{\lambda}}(\mathbf{q}_2), \quad (72)$$

where the color factor is

$$C_{\text{R2},i\bar{i}}^a(\mathbf{q}_2) = \int d^2\mathbf{x} d^2\mathbf{y} e^{-i(\mathbf{k}_q + \mathbf{k}_{\bar{q}} + \mathbf{k}_g - \mathbf{q}_2) \cdot \mathbf{x}} e^{-i\mathbf{q}_2 \cdot \mathbf{y}} [t^a V(\mathbf{x}) V^\dagger(\mathbf{y}) - t^a]_{i\bar{i}}. \quad (73)$$

The perturbative factor for longitudinally polarized photons is

$$\mathcal{J}_{\text{R2},\sigma\bar{\sigma}}^{\lambda=0,\bar{\lambda}}(\mathbf{q}_2) = e e_f g \frac{4Q(1-z_{\bar{q}})z_{\bar{q}}\epsilon^{\bar{\lambda}*n}\bar{u}_\sigma(k_q) \left\{ (z_q \mathbf{k}_g - z_g \mathbf{k}_q)^m \left[\delta^{mn} \left(1 + \frac{z_g}{2z_q} \right) - \frac{z_g}{2z_q} \omega^{mn} \right] \right\} \gamma^+ v_{\bar{\sigma}}(k_{\bar{q}})}{[(1-z_{\bar{q}})z_{\bar{q}}Q^2 + (\mathbf{q}_2 - \mathbf{k}_{\bar{q}})^2] \left[\frac{1}{z_q} (z_q \mathbf{k}_g - z_g \mathbf{k}_q)^2 \right]}, \quad (74)$$

and for transversely polarized photons

$$\begin{aligned} \mathcal{J}_{\text{R2},\sigma\bar{\sigma}}^{\lambda=\pm 1,\bar{\lambda}}(\mathbf{q}_2) = & -e e_f g \frac{2\epsilon^{\bar{\lambda}*n}\epsilon^{\lambda,k}\bar{u}_\sigma(k_q) \left\{ (z_q \mathbf{k}_g - z_g \mathbf{k}_q)^m \left[\delta^{mn} \left(1 + \frac{z_g}{2z_q} \right) - \frac{z_g}{2z_q} \omega^{mn} \right] \right\}}{[(1-z_{\bar{q}})z_{\bar{q}}Q^2 + (\mathbf{q}_2 - \mathbf{k}_{\bar{q}})^2] \left[\frac{1}{z_q} (z_q \mathbf{k}_g - z_g \mathbf{k}_q)^2 \right]} \\ & \times \{ (\mathbf{q}_2 - \mathbf{k}_{\bar{q}})_j [\delta^{kj}(2z_{\bar{q}} - 1) + \omega^{kj}] \} \gamma^+ v_{\bar{\sigma}}(k_{\bar{q}}). \end{aligned} \quad (75)$$

Gluon emission from the antiquark before the shockwave. To obtain the results for the emission from anti-quark, we apply the following rules [92]:

- Swap the variables of the quark and anti-quark: $\mathbf{k}_q \leftrightarrow \mathbf{k}_{\bar{q}}$, $z_q \leftrightarrow z_{\bar{q}}$, $\mathbf{x} \leftrightarrow \mathbf{y}$. In addition, to stick to our convention, we also swap the integration variables: $\mathbf{q}_1 \leftrightarrow \mathbf{q}_2$.
- Write the gamma matrices in reverse order.
- Complex conjugate the color correlator.
- Add an overall “minus” sign.

We can then write the amplitude $\overline{\text{R1}}$ for gluon emission after the shock wave as

$$\mathcal{M}_{\overline{\text{R1}},i\bar{i}}^{\lambda\bar{\lambda},\sigma\bar{\sigma},a}(k_q, k_{\bar{q}}, k_g) = \int \frac{d^2\mathbf{q}_1}{(2\pi)^2} \int \frac{d^2\mathbf{q}_2}{(2\pi)^2} C_{\overline{\text{R1}},i\bar{i}}^a(\mathbf{q}_1, \mathbf{q}_2) \mathcal{J}_{\overline{\text{R1}},\sigma\bar{\sigma}}^{\lambda\bar{\lambda}}(\mathbf{q}_1, \mathbf{q}_2), \quad (76)$$

where the color factor is

$$\begin{aligned} C_{\overline{\text{R1}},i\bar{i}}^a(\mathbf{q}_1, \mathbf{q}_2) = & \int d^2\mathbf{x} d^2\mathbf{y} d^2\mathbf{z} e^{-i\mathbf{q}_1 \cdot \mathbf{x}} e^{-i\mathbf{q}_2 \cdot \mathbf{y}} e^{-i(\mathbf{k}_q + \mathbf{k}_{\bar{q}} + \mathbf{k}_g - \mathbf{q}_1 - \mathbf{q}_2) \cdot \mathbf{z}} \\ & \times [V(\mathbf{x}) V^\dagger(\mathbf{z}) t^a V(\mathbf{z}) V^\dagger(\mathbf{y}) - t^a]_{i\bar{i}}. \end{aligned} \quad (77)$$

and the perturbative factor for longitudinally polarized photon is

$$\begin{aligned} \mathcal{J}_{\overline{\text{R1}},\sigma\bar{\sigma}}^{\lambda=0,\bar{\lambda}}(\mathbf{q}_1, \mathbf{q}_2) = & e e_f g \frac{4Qz_q(1-z_q)\epsilon^{\bar{\lambda}*n}\bar{u}_\sigma(k_q) \left\{ \left(\mathbf{q}_2 - \mathbf{k}_{\bar{q}} + \frac{z_{\bar{q}}}{1-z_q}(\mathbf{q}_1 - \mathbf{k}_q) \right)^m \left[\left(1 + \frac{z_g}{2z_{\bar{q}}} \right) \delta^{mn} + \frac{z_g}{2z_{\bar{q}}} \omega^{mn} \right] \right\} \gamma^+ v_{\bar{\sigma}}(k_{\bar{q}})}{z_g \left[Q^2 z_q(1-z_q) + (\mathbf{q}_1 - \mathbf{k}_q)^2 \right] \left[Q^2 + \frac{(\mathbf{q}_1 - \mathbf{k}_q)^2}{z_q} + \frac{(\mathbf{q}_1 + \mathbf{q}_2 - \mathbf{k}_q - \mathbf{k}_{\bar{q}})^2}{z_g} + \frac{(\mathbf{q}_2 - \mathbf{k}_{\bar{q}})^2}{z_{\bar{q}}} \right]}, \end{aligned} \quad (78)$$

and

$$\begin{aligned} \mathcal{J}_{\overline{\text{R1}},\sigma\bar{\sigma}}^{\lambda=\pm 1,\bar{\lambda}}(\mathbf{q}_1, \mathbf{q}_2) = & \frac{e e_f g \epsilon^{\bar{\lambda}*n}\epsilon^{\lambda,k}}{\left[Q^2 + \frac{(\mathbf{q}_1 - \mathbf{k}_q)^2}{z_q} + \frac{(\mathbf{q}_1 + \mathbf{q}_2 - \mathbf{k}_q - \mathbf{k}_{\bar{q}})^2}{z_g} + \frac{(\mathbf{q}_2 - \mathbf{k}_{\bar{q}})^2}{z_{\bar{q}}} \right]} \\ & \times \bar{u}_\sigma(k_q) \left\{ (\mathbf{q}_1 - \mathbf{k}_q)^j [\delta^{kj}(1-2z_q) + \omega^{kj}] \right\} \\ & \times \frac{2 \left\{ \left(\mathbf{q}_2 - \mathbf{k}_{\bar{q}} + \frac{z_{\bar{q}}}{1-z_q}(\mathbf{q}_1 - \mathbf{k}_q) \right)^m \left[\left(1 + \frac{z_g}{2z_{\bar{q}}} \right) \delta^{mn} + \frac{z_g}{2z_{\bar{q}}} \omega^{mn} \right] \right\}}{z_g [Q^2 z_q(1-z_q) + (\mathbf{q}_1 - \mathbf{k}_q)^2]} + \frac{\gamma^k \gamma^n}{(1-z_q)} \gamma^+ v_{\bar{\sigma}}(k_{\bar{q}}), \end{aligned} \quad (79)$$

for transversely polarized photons.

Gluon emission from the antiquark after the shockwave. Finally, to obtain the amplitude for the emission from antiquark after the shockwave, we proceed similarly and apply the following rules:

- Swap the variables of the quark and anti-quark: $k_q \leftrightarrow k_{\bar{q}}, z_q \leftrightarrow z_{\bar{q}}, x \leftrightarrow y$. In addition, to stick to our convention, we also swap the integration variables: $q_2 \leftrightarrow k_q + k_{\bar{q}} + k_g - q_2$.
- Write the gamma matrices in reverse order.
- Complex conjugate the color correlator.
- Add an overall “minus” sign.

The amplitude $\overline{\text{R2}}$ reads then

$$\mathcal{M}_{\overline{\text{R2}}, i\bar{i}}^{\lambda\bar{\lambda}, \sigma\bar{\sigma}, a}(k_q, k_{\bar{q}}, k_g) = \int \frac{d^2 q_2}{(2\pi)^2} C_{\overline{\text{R2}}, i\bar{i}}^a(q_2) \mathcal{J}_{\overline{\text{R1}}, \sigma\bar{\sigma}}^{\lambda\bar{\lambda}}(q_2), \quad (80)$$

where the color factor is

$$C_{\overline{\text{R2}}, i\bar{i}}^a(q_2) = \int d^2 x d^2 y e^{-i(k_q + k_{\bar{q}} + k_g - q_2) \cdot x} e^{-i q_2 \cdot y} [V(x) V^\dagger(y) t^a - t^a]_{i\bar{i}}, \quad (81)$$

and the perturbative factor for longitudinally polarized virtual photon is

$$\mathcal{J}_{\overline{\text{R2}}, \sigma\bar{\sigma}}^{\lambda=0, \bar{\lambda}}(q_2) = -e e_f g \frac{4Q(1-z_q)z_q \epsilon^{\bar{\lambda}*, n} \bar{u}_\sigma(k_q) \left\{ (z_{\bar{q}} k_g - z_g k_{\bar{q}})^m \left[\delta^{mn} \left(1 + \frac{z_g}{2z_{\bar{q}}} \right) + \frac{z_g}{2z_{\bar{q}}} \omega^{mn} \right] \right\} \gamma^+ v_{\bar{\sigma}}(k_{\bar{q}})}{[(1-z_q)z_q Q^2 + (k_{\bar{q}} + k_g - q_2)^2] \left[\frac{1}{z_{\bar{q}}} (z_{\bar{q}} k_g - z_g k_{\bar{q}})^2 \right]}, \quad (82)$$

while it is given by

$$\begin{aligned} \mathcal{J}_{\overline{\text{R2}}, \sigma\bar{\sigma}}^{\lambda=\pm 1, \bar{\lambda}}(q_2) &= e e_f g \frac{2\epsilon^{\bar{\lambda}*, n} \epsilon^{\lambda, k} \bar{u}_\sigma(k_q) \left\{ (k_{\bar{q}} + k_g - q_2)_j \left[\delta^{kj} (2z_q - 1) - \omega^{kj} \right] \right\}}{[(1-z_q)z_q Q^2 + (k_{\bar{q}} + k_g - q_2)^2] \left[\frac{1}{z_{\bar{q}}} (z_{\bar{q}} k_g - z_g k_{\bar{q}})^2 \right]} \\ &\times \left\{ (z_{\bar{q}} k_g - z_g k_{\bar{q}})^m \left[\delta^{mn} \left(1 + \frac{z_g}{2z_{\bar{q}}} \right) + \frac{z_g}{2z_{\bar{q}}} \omega^{mn} \right] \right\} \gamma^+ v_{\bar{\sigma}}(k_{\bar{q}}), \end{aligned} \quad (83)$$

for transversely polarized photons.

Amplitudes: extracting the leading power in K_\perp/P_\perp and Q_s/P_\perp

In this section, we extract the leading power contribution in K_\perp/P_\perp and Q_s/P_\perp to the amplitudes derived in the previous section. We will then demonstrate that the integral over the phase space of the unobserved antiquark is dominated by values $z_{\bar{q}} \lesssim K_\perp^2/P_\perp^2 \ll 1$. Our goal is thus to demonstrate Eq. (2) in the main text.

The back-to-back limit of interest corresponds to

$$Q_s, |K| \ll |P|. \quad (84)$$

Due to our choice of momenta definition, q_1 and q_2 correspond to the momenta transfer from the shockwave to the quark and antiquark, respectively. Their magnitudes are controlled by the intrinsic saturation scale Q_s . Thus, the condition $Q_s \ll |P|$ implies that

$$|q_1|, |q_2| \sim Q_s \ll |P|. \quad (85)$$

Furthermore, we expect the total momentum transfer of the shockwave to the three-parton system to be of order of the saturation scale; hence

$$|k_{\bar{q}} + K| \sim Q_s \ll |P| \rightarrow |k_{\bar{q}}| \ll |P|. \quad (86)$$

Therefore, in the back-to-back limit of quark-gluon jets we have the hierarchy of scales:

$$|\mathbf{q}_1|, |\mathbf{q}_2|, |\mathbf{k}_{\bar{q}}| \ll |\mathbf{P}| \sim |\mathbf{k}_q| \sim |\mathbf{k}_{\bar{q}}|. \quad (87)$$

Let us perform the leading power expansion of the perturbative factors in Eqs. (69)-(74)-(78)-(82) in the longitudinally polarized photon case and Eqs. (70)-(75)-(79)-(83) in the transversely polarized photon case, according to the hierarchy of scales in Eq. (87).

For longitudinally polarized photons, we find

$$\mathcal{J}_{\text{R1},\sigma\bar{\sigma}}^{\lambda=0,\bar{\lambda}}(\mathbf{q}_2) = \frac{ee_f g z_{\bar{q}}^2 (1 - z_{\bar{q}})}{z_q z_g} \frac{2Q \epsilon^{\bar{\lambda}*n}(\mathbf{P})^m \bar{u}_\sigma(k_q) [(2z_q + z_g) \delta^{mn} - z_g \omega^{mn}] \gamma^+ v_{\bar{\sigma}}(k_{\bar{q}})}{[z_{\bar{q}}(1 - z_{\bar{q}})Q^2 + (\mathbf{q}_2 - \mathbf{k}_{\bar{q}})^2] \left[z_{\bar{q}} \left(Q^2 + \frac{\mathbf{P}^2}{z_q z_g} \right) + (\mathbf{q}_2 - \mathbf{k}_{\bar{q}})^2 \right]}, \quad (88)$$

$$\mathcal{J}_{\text{R2},\sigma\bar{\sigma}}^{\lambda=0,\bar{\lambda}}(\mathbf{q}_2) = -\frac{ee_f g z_{\bar{q}}^2}{z_q z_g} \frac{2Q \epsilon^{\bar{\lambda}*n}(\mathbf{P})^m \bar{u}_\sigma(k_q) [(2z_q + z_g) \delta^{mn} - z_g \omega^{mn}] \gamma^+ v_{\bar{\sigma}}(k_{\bar{q}})}{[z_{\bar{q}}(1 - z_{\bar{q}})Q^2 + (\mathbf{q}_2 - \mathbf{k}_{\bar{q}})^2] \left[z_{\bar{q}} \frac{\mathbf{P}^2}{z_q z_g} \right]}, \quad (89)$$

$$\mathcal{J}_{\text{R1},\sigma\bar{\sigma}}^{\lambda=0,\bar{\lambda}}(\mathbf{q}_2) = ee_f g z_q (1 - z_q) \frac{2Q \epsilon^{\bar{\lambda}*n} \left(\mathbf{q}_2 - \mathbf{k}_{\bar{q}} - \frac{z_{\bar{q}}}{1 - z_q} \mathbf{P} \right)^m \bar{u}_\sigma(k_q) \left[\left(\frac{2z_{\bar{q}}}{z_g} + 1 \right) \delta^{mn} + \omega^{mn} \right] \gamma^+ v_{\bar{\sigma}}(k_{\bar{q}})}{[z_q(1 - z_q)Q^2 + \mathbf{P}^2] \left[z_{\bar{q}} \left(Q^2 + \frac{\mathbf{P}^2}{z_q z_g} \right) + (\mathbf{q}_2 - \mathbf{k}_{\bar{q}})^2 \right]}, \quad (90)$$

$$\mathcal{J}_{\text{R2},\sigma\bar{\sigma}}^{\lambda=0,\bar{\lambda}} = \frac{ee_f g z_q (1 - z_q)}{z_g} \frac{2Q \epsilon^{\bar{\lambda}*n} (z_{\bar{q}} \mathbf{P} + z_g \mathbf{k}_{\bar{q}})^m \bar{u}_\sigma(k_q) \left[\left(\frac{2z_{\bar{q}}}{z_g} + 1 \right) \delta^{mn} + \omega^{mn} \right] \gamma^+ v_{\bar{\sigma}}(k_{\bar{q}})}{[z_q(1 - z_q)Q^2 + \mathbf{P}^2] [(z_{\bar{q}} \mathbf{P} + z_g \mathbf{k}_{\bar{q}})^2]}. \quad (91)$$

For transversely polarized photons, we find

$$\begin{aligned} \mathcal{J}_{\text{R1},\sigma\bar{\sigma}}^{\lambda=\pm 1,\bar{\lambda}}(\mathbf{q}_2) &= \frac{ee_f g z_{\bar{q}}}{z_q z_g} \frac{\epsilon^{\bar{\lambda}*n} \epsilon^{\lambda,k}}{\left[z_{\bar{q}} \left(Q^2 + \frac{\mathbf{P}^2}{z_q z_g} \right) + (\mathbf{q}_2 - \mathbf{k}_{\bar{q}})^2 \right]} \\ &\times \bar{u}_\sigma(k_q) \left[\frac{(\mathbf{P})^m (\mathbf{q}_2 - \mathbf{k}_{\bar{q}})^j [(2z_q + z_g) \delta^{mn} - z_g \omega^{mn}] [\delta^{kj}(1 - 2z_{\bar{q}}) - \omega^{kj}]}{[z_{\bar{q}}(1 - z_{\bar{q}})Q^2 + (\mathbf{q}_2 - \mathbf{k}_{\bar{q}})^2]} - \frac{z_q \gamma^n \gamma^k}{(1 - z_q)} \right] \gamma^+ v_{\bar{\sigma}}(k_{\bar{q}}), \end{aligned} \quad (92)$$

$$\begin{aligned} \mathcal{J}_{\text{R2},\sigma\bar{\sigma}}^{\lambda=\pm 1,\bar{\lambda}}(\mathbf{q}_2) &= -\frac{ee_f g z_{\bar{q}}}{z_q z_g (1 - z_{\bar{q}})} \frac{\epsilon^{\bar{\lambda}*n} \epsilon^{\lambda,k}}{\left[z_{\bar{q}} \frac{\mathbf{P}^2}{z_q z_g} \right]} \\ &\times \frac{\bar{u}_\sigma(k_q) (\mathbf{P})^m (\mathbf{q}_2 - \mathbf{k}_{\bar{q}})_j [(2z_q + z_g) \delta^{mn} - z_g \omega^{mn}] [\delta^{kj}(1 - 2z_{\bar{q}}) - \omega^{kj}] \gamma^+ v_{\bar{\sigma}}(k_{\bar{q}})}{[z_{\bar{q}}(1 - z_{\bar{q}})Q^2 + (\mathbf{q}_2 - \mathbf{k}_{\bar{q}})^2]}, \end{aligned} \quad (93)$$

$$\begin{aligned} \mathcal{J}_{\text{R1},\sigma\bar{\sigma}}^{\lambda=\pm 1,\bar{\lambda}}(\mathbf{q}_2) &= -ee_f g \frac{\epsilon^{\bar{\lambda}*n} \epsilon^{\lambda,k}}{\left[z_{\bar{q}} \left(Q^2 + \frac{\mathbf{P}^2}{z_q z_g} \right) + (\mathbf{q}_2 - \mathbf{k}_{\bar{q}})^2 \right]} \\ &\times \bar{u}_\sigma(k_q) \left\{ \frac{(\mathbf{P})^j \left(\mathbf{q}_2 - \mathbf{k}_{\bar{q}} - \frac{z_{\bar{q}}}{1 - z_q} \mathbf{P} \right)^m [\delta^{kj}(1 - 2z_q) + \omega^{kj}] \left[\left(\frac{2z_{\bar{q}}}{z_g} + 1 \right) \delta^{mn} + \omega^{mn} \right]}{[z_q(1 - z_q)Q^2 + \mathbf{P}^2]} + \frac{z_{\bar{q}} \gamma^k \gamma^n}{(1 - z_q)} \right\} \gamma^+ v_{\bar{\sigma}}(k_{\bar{q}}), \end{aligned} \quad (94)$$

$$\mathcal{J}_{\text{R2},\sigma\bar{\sigma}}^{\lambda=\pm 1,\bar{\lambda}} = ee_f g \frac{\epsilon^{\bar{\lambda}*n} \epsilon^{\lambda,k} \bar{u}_\sigma(k_q) (\mathbf{P})_j (z_{\bar{q}} \mathbf{P} + z_g \mathbf{k}_{\bar{q}})^m [\delta^{kj}(2z_q - 1) - \omega^{kj}] [\delta^{mn}(2z_{\bar{q}} + z_g) + z_g \omega^{mn}] \gamma^+ v_{\bar{\sigma}}(k_{\bar{q}})}{[z_q(1 - z_q)Q^2 + \mathbf{P}^2] [(z_{\bar{q}} \mathbf{P} + z_g \mathbf{k}_{\bar{q}})^2]}. \quad (95)$$

We observe that for both polarizations amplitudes R1, R2 and $\overline{\text{R1}}$ are independent of \mathbf{q}_1 , while $\overline{\text{R2}}$ is independent of \mathbf{q}_1 and \mathbf{q}_2 . Hence, we can write the total amplitude at leading power as

$$\begin{aligned} \mathcal{M}_{qg(\bar{q}),\sigma\bar{\sigma},i\bar{i}}^{\lambda\bar{\lambda},a} &= \int \frac{d^2 \mathbf{q}_2}{(2\pi)^2} \left\{ \left[\mathcal{J}_{\text{R1},\sigma\bar{\sigma}}^{\lambda\bar{\lambda}}(\mathbf{q}_2) + \mathcal{J}_{\text{R1},\sigma\bar{\sigma}}^{\lambda\bar{\lambda}}(\mathbf{q}_2) \right] \int \frac{d^2 \mathbf{q}_1}{(2\pi)^2} \mathcal{C}_{\text{R1},i\bar{i}}^a(\mathbf{q}_1, \mathbf{q}_2) + \mathcal{J}_{\text{R2},\sigma\bar{\sigma}}^{\lambda\bar{\lambda}}(\mathbf{q}_2) \mathcal{C}_{\text{R2},i\bar{i}}^a(\mathbf{q}_2) \right\} \\ &+ \mathcal{J}_{\text{R2},\sigma\bar{\sigma}}^{\lambda\bar{\lambda}} \int \frac{d^2 \mathbf{q}_2}{(2\pi)^2} \mathcal{C}_{\text{R2},i\bar{i}}^a(\mathbf{q}_2). \end{aligned} \quad (96)$$

Due to unitarity of the Wilson lines, we observe the contribution from $\overline{\text{R2}}$ vanishes:

$$\int \frac{d^2 \mathbf{q}_2}{(2\pi)^2} \mathcal{C}_{\text{R2},i\bar{i}}^a(\mathbf{q}_2) = \int \frac{d^2 \mathbf{q}_2}{(2\pi)^2} \int d^2 x d^2 y e^{-i \mathbf{q}_2 \cdot \mathbf{y}} e^{-i(\mathbf{K} + \mathbf{k}_{\bar{q}} - \mathbf{q}_2) \cdot \mathbf{x}} [V(\mathbf{x}) V^\dagger(\mathbf{y}) t^a - t^a]_{i\bar{i}} \quad (97)$$

$$= \int d^2 x e^{-i(\mathbf{k}_q + \mathbf{k}_{\bar{q}} + \mathbf{k}_g) \cdot \mathbf{x}} [V(\mathbf{x}) V^\dagger(\mathbf{x}) t^a - t^a]_{i\bar{i}} = 0. \quad (98)$$

Meanwhile, the color operator corresponding to the emission before the shockwave simplifies to that of the emission after the shockwave from the quark

$$\begin{aligned}
\int \frac{d^2 \mathbf{q}_1}{(2\pi)^2} C_{R1, i\bar{i}}^a(\mathbf{q}_1, \mathbf{q}_2) &= \int \frac{d^2 \mathbf{q}_1}{(2\pi)^2} \int d^2 \mathbf{x} d^2 \mathbf{y} d^2 \mathbf{z} e^{-i \mathbf{q}_1 \cdot \mathbf{x}} e^{-i \mathbf{q}_2 \cdot \mathbf{y}} e^{-i(\mathbf{K} + \mathbf{k}_{\bar{q}} - \mathbf{q}_1 - \mathbf{q}_2) \cdot \mathbf{z}} \\
&\times [V(\mathbf{x}) V^\dagger(\mathbf{z}) t^a V(\mathbf{z}) V^\dagger(\mathbf{y}) - t^a]_{i\bar{i}} \\
&= \int d^2 \mathbf{x} d^2 \mathbf{y} e^{-i \mathbf{q}_2 \cdot \mathbf{y}} e^{-i(\mathbf{K} + \mathbf{k}_{\bar{q}} - \mathbf{q}_2) \cdot \mathbf{x}} [t^a V(\mathbf{x}) V^\dagger(\mathbf{y}) - t^a]_{i\bar{i}} \\
&= C_{R2, i\bar{i}}^a(\mathbf{q}_2).
\end{aligned} \tag{99}$$

One can therefore write the sum of the four amplitudes in a very compact form involving only the color operator associated with a gluon emission by the quark after the shockwave:

$$\mathcal{M}_{qg(\bar{q}), \sigma\bar{\sigma}, i\bar{i}}^{\lambda\bar{\lambda}, a} = \int \frac{d^2 \mathbf{q}_2}{(2\pi)^2} [\mathcal{J}_{q, \sigma\bar{\sigma}}^{\lambda\bar{\lambda}}(\mathbf{q}_2) + \mathcal{J}_{\bar{q}, \sigma\bar{\sigma}}^{\lambda\bar{\lambda}}(\mathbf{q}_2)] C_{R2, i\bar{i}}^a(\mathbf{q}_2), \tag{100}$$

where we have conveniently defined the contributions from quark and antiquark emissions

$$\mathcal{J}_{q, \sigma\bar{\sigma}}^{\lambda\bar{\lambda}}(\mathbf{q}_2) = \mathcal{J}_{R1, \sigma\bar{\sigma}}^{\lambda=, \bar{\lambda}}(\mathbf{q}_2) + \mathcal{J}_{R2, \sigma\bar{\sigma}}^{\lambda=, \bar{\lambda}}(\mathbf{q}_2), \tag{101}$$

$$\mathcal{J}_{\bar{q}, \sigma\bar{\sigma}}^{\lambda\bar{\lambda}}(\mathbf{q}_2) = \mathcal{J}_{R1, \sigma\bar{\sigma}}^{\lambda=, \bar{\lambda}}(\mathbf{q}_2). \tag{102}$$

For longitudinally polarized photons, we find

$$\begin{aligned}
\mathcal{J}_{q, \sigma\bar{\sigma}}^{\lambda=0, \bar{\lambda}}(\mathbf{q}_2) &= -e e_f g z_{\bar{q}} \frac{2Q \epsilon^{\bar{\lambda}*, n}(\mathbf{P})^m \bar{u}_\sigma(k_q) [(2z_q + z_g) \delta^{mn} - z_g \omega^{mn}] \gamma^+ v_{\bar{\sigma}}(k_{\bar{q}})}{P^2 \left[z_{\bar{q}} \left(Q^2 + \frac{P^2}{z_q z_g} \right) + (\mathbf{q}_2 - \mathbf{k}_{\bar{q}})^2 \right]} \\
&\times \left[\frac{[z_{\bar{q}} Q^2 + (\mathbf{q}_2 - \mathbf{k}_{\bar{q}})^2]}{[z_{\bar{q}}(1 - z_{\bar{q}}) Q^2 + (\mathbf{q}_2 - \mathbf{k}_{\bar{q}})^2]} + \frac{z_{\bar{q}}^2 P^2}{z_q z_g [z_{\bar{q}}(1 - z_{\bar{q}}) Q^2 + (\mathbf{q}_2 - \mathbf{k}_{\bar{q}})^2]} \right],
\end{aligned} \tag{103}$$

$$\mathcal{J}_{\bar{q}, \sigma\bar{\sigma}}^{\lambda=0, \bar{\lambda}}(\mathbf{q}_2) = e e_f g z_q (1 - z_q) \frac{2Q \epsilon^{\bar{\lambda}*, n} \left(\mathbf{q}_2 - \mathbf{k}_{\bar{q}} + \frac{z_{\bar{q}}}{1 - z_q}(\mathbf{P}) \right)^m \bar{u}_\sigma(k_q) \left[\left(\frac{2z_{\bar{q}}}{z_g} + 1 \right) \delta^{mn} + \omega^{mn} \right] \gamma^+ v_{\bar{\sigma}}(k_{\bar{q}})}{[z_q(1 - z_q) Q^2 + P^2] \left[z_{\bar{q}} \left(Q^2 + \frac{P^2}{z_q z_g} \right) + (\mathbf{q}_2 - \mathbf{k}_{\bar{q}})^2 \right]}. \tag{104}$$

For transversely polarized photons, we find

$$\begin{aligned}
\mathcal{J}_{q, \sigma\bar{\sigma}}^{\lambda=\pm 1, \bar{\lambda}}(\mathbf{q}_2) &= -e e_f g \frac{\epsilon^{\bar{\lambda}*, n} \epsilon^{\lambda, k}}{\left[z_{\bar{q}} \left(Q^2 + \frac{P^2}{z_q z_g} \right) + (\mathbf{q}_2 - \mathbf{k}_{\bar{q}})^2 \right]} \\
&\times \bar{u}_\sigma(k_q) \left\{ \frac{[z_{\bar{q}} Q^2 + (\mathbf{q}_2 - \mathbf{k}_{\bar{q}})^2]}{[z_{\bar{q}}(1 - z_{\bar{q}}) Q^2 + (\mathbf{q}_2 - \mathbf{k}_{\bar{q}})^2]} \frac{(\mathbf{P})^m (\mathbf{q}_2 - \mathbf{k}_{\bar{q}})^j [(2z_q + z_g) \delta^{mn} - z_g \omega^{mn}] [\delta^{kj}(1 - 2z_{\bar{q}}) - \omega^{kj}]}{P^2} \right. \\
&\left. + \frac{z_{\bar{q}} z_q \gamma^n \gamma^k}{z_q z_g (1 - z_{\bar{q}})} \right\} \gamma^+ v_{\bar{\sigma}}(k_{\bar{q}}),
\end{aligned} \tag{105}$$

$$\begin{aligned}
\mathcal{J}_{\bar{q}, \sigma\bar{\sigma}}^{\lambda=\pm 1, \bar{\lambda}}(\mathbf{q}_2) &= - \frac{e e_f g \epsilon^{\bar{\lambda}*, n} \epsilon^{\lambda, k}}{\left[z_{\bar{q}} \left(Q^2 + \frac{P^2}{z_q z_g} \right) + (\mathbf{q}_2 - \mathbf{k}_{\bar{q}})^2 \right]} \\
&\times \bar{u}_\sigma(k_q) \left\{ \frac{(\mathbf{P})^j \left(\mathbf{q}_2 - \mathbf{k}_{\bar{q}} - \frac{z_{\bar{q}}}{1 - z_q} \mathbf{P} \right)^m [\delta^{kj}(1 - 2z_q) + \omega^{kj}]}{[z_q(1 - z_q) Q^2 + P^2]} \left[\left(\frac{2z_{\bar{q}}}{z_g} + 1 \right) \delta^{mn} + \omega^{mn} \right] + \frac{z_{\bar{q}} \gamma^k \gamma^n}{(1 - z_q)} \right\} \gamma^+ v_{\bar{\sigma}}(k_{\bar{q}}).
\end{aligned} \tag{106}$$

We observe that all perturbative factors are proportional to

$$\frac{1}{\left[z_{\bar{q}} \left(Q^2 + \frac{P^2}{z_q z_g} \right) + (\mathbf{q}_2 - \mathbf{k}_{\bar{q}})^2 \right]}. \tag{107}$$

In order to compensate for the large values of P^2 , the integration over $z_{\bar{q}}$ is dominated by small values

$$z_{\bar{q}} \lesssim z_q z_g (\mathbf{q}_2 - \mathbf{k}_{\bar{q}})^2 / (z_q z_g Q^2 + P^2) \sim \max(Q_s^2, K^2) / P^2 \ll 1. \quad (108)$$

Thus we see that the leading power contribution in the back-to-back limit demands the unobserved antiquark to have small momentum fraction, and the observed quark and gluon jets carry the total longitudinal momentum of the virtual photon. This is analogous to the dominance of the aligned jet configuration in SIDIS at high Q^2 .

Expanding the hard factors around small $z_{\bar{q}}$, we find for the longitudinally polarized case

$$\mathcal{J}_{q,\sigma\bar{\sigma}}^{\lambda=0,\bar{\lambda}}(\mathbf{q}_2) = 0 \quad (\text{power suppressed}), \quad (109)$$

$$\begin{aligned} \mathcal{J}_{q,\sigma\bar{\sigma}}^{\lambda=0,\bar{\lambda}}(\mathbf{q}_2) &= ee_f g z_q z_g \frac{2Q \epsilon^{\bar{\lambda}*,n}(\mathbf{q}_2 - \mathbf{k}_{\bar{q}})^m \bar{u}_\sigma(k_q) [\delta^{mn} + \omega^{mn}] \gamma^+ v_{\bar{\sigma}}(k_{\bar{q}})}{[z_q z_g Q^2 + P^2] \left[(\mathbf{q}_2 - \mathbf{k}_{\bar{q}})^2 + z_{\bar{q}} \left(Q^2 + \frac{P^2}{z_q z_g} \right) \right]} \\ &= 8ee_f g \sqrt{z_q z_{\bar{q}}} q^+ \delta^{\sigma,-\bar{\sigma}} \delta^{\sigma,\bar{\lambda}} \frac{Q(\mathbf{q}_2 - \mathbf{k}_{\bar{q}}) \cdot \epsilon^{\bar{\lambda}*}}{[z_{\bar{q}}(Q^2 + M_{qg}^2) + (\mathbf{q}_2 - \mathbf{k}_{\bar{q}})^2] [Q^2 + M_{qg}^2]}, \end{aligned} \quad (110)$$

and for the transversely polarized case

$$\begin{aligned} \mathcal{J}_{q,\sigma\bar{\sigma}}^{\lambda=\pm 1,\bar{\lambda}}(\mathbf{q}_2) &= -ee_f g \frac{\epsilon^{\bar{\lambda}*,n} \epsilon^{\lambda,k}(P)^m (\mathbf{q}_2 - \mathbf{k}_{\bar{q}})^j \bar{u}_\sigma(k_q) [(1 + z_q) \delta^{mn} - z_g \omega^{mn}] [\delta^{kj} - \omega^{kj}] \gamma^+ v_{\bar{\sigma}}(k_{\bar{q}})}{P^2 \left[z_{\bar{q}} \left(Q^2 + \frac{P^2}{z_q z_g} \right) + (\mathbf{q}_2 - \mathbf{k}_{\bar{q}})^2 \right]} \\ &= -8ee_f g \sqrt{z_q z_{\bar{q}}} q^+ \delta^{\sigma,-\bar{\sigma}} \delta^{\sigma,-\lambda} \left[\delta^{\lambda\bar{\lambda}} + z_q \delta^{\lambda,-\bar{\lambda}} \right] \frac{(P \cdot \epsilon^{\bar{\lambda}*)} ((\mathbf{q}_2 - \mathbf{k}_{\bar{q}}) \cdot \epsilon^\lambda)}{z_q z_g M_{qg}^2 [(\mathbf{q}_2 - \mathbf{k}_{\bar{q}})^2 + z_{\bar{q}}(Q^2 + M_{qg}^2)]}, \end{aligned} \quad (111)$$

$$\begin{aligned} \mathcal{J}_{q,\sigma\bar{\sigma}}^{\lambda=\pm 1,\bar{\lambda}}(\mathbf{q}_2) &= -ee_f g \frac{\epsilon^{\bar{\lambda}*,n} \epsilon^{\lambda,k}(P)^j (\mathbf{q}_2 - \mathbf{k}_{\bar{q}})^m \bar{u}_\sigma(k_q) [\delta^{kj}(1 - 2z_q) + \omega^{kj}] [\delta^{mn} + \omega^{mn}] \gamma^+ v_{\bar{\sigma}}(k_{\bar{q}})}{[z_q(1 - z_q)Q^2 + P^2] \left[z_{\bar{q}} \left(Q^2 + \frac{P^2}{z_q z_g} \right) + (\mathbf{q}_2 - \mathbf{k}_{\bar{q}})^2 \right]} \\ &= -8ee_f g \sqrt{z_q z_{\bar{q}}} q^+ \delta^{\sigma,-\bar{\sigma}} \delta^{\sigma,\bar{\lambda}} \left[z_g \delta^{\lambda,\bar{\lambda}} - z_q \delta^{\lambda,-\bar{\lambda}} \right] \frac{(P \cdot \epsilon^\lambda) ((\mathbf{q}_2 - \mathbf{k}_{\bar{q}}) \cdot \epsilon^{\bar{\lambda}*)}}{z_q z_g [M_{qg}^2 + Q^2] [(\mathbf{q}_2 - \mathbf{k}_{\bar{q}})^2 + z_{\bar{q}}(Q^2 + M_{qg}^2)]}. \end{aligned} \quad (112)$$

Here we have introduced the dijet invariant mass $M_{qg}^2 = P_\perp^2 / (z_q z_g)$. One notices that for longitudinally polarized virtual photons, only diagram $\overline{\text{R1}}$ (gluon emission from antiquark before the shockwave) contributes to the back-to-back limit of inclusive quark-gluon jet production in DIS. In each second line of the above equations, the helicity and polarization dependence is shown explicitly in order to simplify the calculation of the helicity-polarization sum at the cross-section level.

To make the connection with the results displayed in the main text, we introduce the same notations, and in particular the operator $\mathcal{C}_{1,i\bar{i}}^a$ defined in Eq. (3) of the main text as

$$\mathcal{C}_{1,i\bar{i}}^a(\mathbf{q}_1, \mathbf{q}_2) = \int d^2x d^2y e^{-i\mathbf{q}_1 \cdot \mathbf{x} - i\mathbf{q}_2 \cdot \mathbf{y}} [t^a V(\mathbf{x}) V^\dagger(\mathbf{y}) - t^a]_{i\bar{i}}. \quad (113)$$

Performing the change of variable $\ell = \mathbf{q}_2 - \mathbf{k}_{\bar{q}}$, we get the following compact results for the sum of all amplitudes:

$$\begin{aligned} \mathcal{M}_{qg(\bar{q}),\sigma\bar{\sigma},i\bar{i}}^{\lambda=\pm 1,\bar{\lambda},a} &= -8ee_f g \sqrt{z_q z_{\bar{q}}} q^+ \delta^{\sigma,-\bar{\sigma}} \int \frac{d^2\ell}{(2\pi)^2} \frac{1}{\ell^2 + z_{\bar{q}}(Q^2 + M_{qg}^2)} \mathcal{C}_{1,i\bar{i}}^a(\mathbf{K} - \ell, \ell + \mathbf{k}_{\bar{q}}) \\ &\times \frac{1}{z_q z_g} \left\{ \delta^{\sigma,-\lambda} \left[\delta^{\lambda\bar{\lambda}} + z_q \delta^{\lambda,-\bar{\lambda}} \right] \frac{(P \cdot \epsilon^{\bar{\lambda}*)} (\ell \cdot \epsilon^\lambda)}{M_{qg}^2} + \delta^{\sigma,\bar{\lambda}} \left[z_g \delta^{\lambda,\bar{\lambda}} - z_q \delta^{\lambda,-\bar{\lambda}} \right] \frac{(P \cdot \epsilon^\lambda) (\ell \cdot \epsilon^{\bar{\lambda}*)}}{M_{qg}^2 + Q^2} \right\}, \end{aligned} \quad (114)$$

$$\mathcal{M}_{qg(\bar{q}),\sigma\bar{\sigma},i\bar{i}}^{\lambda=0,\bar{\lambda},a} = 8ee_f g \sqrt{z_q z_{\bar{q}}} q^+ \delta^{\sigma,-\bar{\sigma}} \delta^{\bar{\lambda}\sigma} \frac{Q}{M_{qg}^2 + Q^2} \int \frac{d^2\ell}{(2\pi)^2} \frac{\ell \cdot \epsilon^{\bar{\lambda}*}}{\ell^2 + z_{\bar{q}}(Q^2 + M_{qg}^2)} \mathcal{C}_{1,i\bar{i}}^a(\mathbf{K} - \ell, \ell + \mathbf{k}_{\bar{q}}). \quad (115)$$

The last equality is exactly Eq. (2) in the main text of the Letter.

Differential cross-section for inclusive back-back quark-gluon-dijet production in DIS

A useful change of variable

The differential cross-section for inclusive back-to-back quark-gluon production in DIS can be obtained from the amplitude squared using

$$\frac{d\sigma^{\gamma^* A \rightarrow qg+X}}{d^2P d^2K dz_g dz_q} = \frac{1}{16(2\pi)^8 z_q z_g (q^+)^2} \delta(1 - z_q - z_g) \int_0^1 \frac{dz_{\bar{q}}}{z_{\bar{q}}} \int d^2k_{\bar{q}} \sum_{\sigma\bar{\sigma}, i\bar{i}, \bar{\lambda}, a} \left\langle \left| \mathcal{M}_{qg(\bar{q}), \sigma\bar{\sigma}, i\bar{i}}^{\lambda, \bar{\lambda}, a} \right|^2 \right\rangle_{x_g}. \quad (116)$$

The CGC average $\langle \dots \rangle$, as obtained from BK-JIMWLK evolution of the color operator involved in this process and to be specified below, must be evaluated at the scale determined by the target longitudinal momentum fraction of the t -channel gluon participating in the $\gamma^* g \rightarrow qg\bar{q}$ process, namely

$$x_g = \frac{1}{\hat{s}} \left(M_{qg}^2 + Q^2 + \frac{K_{\perp}^2}{z_{\bar{q}}} \right). \quad (117)$$

Let us define the variable ξ ,

$$\xi = \frac{z_{\bar{q}} (M_{qg}^2 + Q^2)}{z_{\bar{q}} (M_{qg}^2 + Q^2) + K^2}. \quad (118)$$

This corresponds to the fraction of longitudinal momentum (with respect to target) of the small- x sea quark relative to the small- x gluon, i.e. $\xi = x/x_g$ with $x = (M_{qg}^2 + Q^2)/\hat{s}$ the target longitudinal momentum fraction of the t -channel quark in the $\gamma^* q \rightarrow qg$ subprocess. For now, we take it as a convenient change of variables in the integral over $z_{\bar{q}}$. Then we can trade $z_{\bar{q}}$ by ξ using

$$z_{\bar{q}} (M_{qg}^2 + Q^2) = \frac{\xi K^2}{(1 - \xi)}, \quad dz_{\bar{q}} = \frac{1}{(1 - \xi)^2} \frac{K^2}{M_{qg}^2 + Q^2} d\xi. \quad (119)$$

We can compactly express the differential cross-section as

$$\frac{d\sigma^{\lambda}}{d^2P d^2K dz_q dz_g} = \int_0^1 d\xi \int d^2k_{\bar{q}} \int \frac{d^2q_2}{(2\pi)^2} \int \frac{d^2q'_{2\perp}}{(2\pi)^2} \Xi(q_2, q'_{2\perp}) \mathcal{H}^{\lambda}(q_2, q'_{2\perp}), \quad (120)$$

where the perturbative factor reads

$$\mathcal{H}^{\lambda}(q_2, q'_{2\perp}) = \frac{\delta(1 - z_q - z_g)}{16(2\pi)^2 (q^+)^2 (1 - \xi)^2} \frac{K^2}{z_{\bar{q}} (P^2 + z_q z_g Q^2)} \sum_{\sigma\bar{\sigma}\bar{\lambda}} \left[\mathcal{J}_{q, \sigma\bar{\sigma}}^{\lambda\bar{\lambda}}(q_2) + \mathcal{J}_{\bar{q}, \sigma\bar{\sigma}}^{\lambda\bar{\lambda}}(q_2) \right] \left[\mathcal{J}_{q, \sigma\bar{\sigma}}^{\lambda\bar{\lambda}}(q'_{2\perp}) + \mathcal{J}_{\bar{q}, \sigma\bar{\sigma}}^{\lambda\bar{\lambda}}(q'_{2\perp}) \right], \quad (121)$$

and the color operator is

$$\begin{aligned} \Xi(q_2, q'_{2\perp}) &= \frac{1}{(2\pi)^6} \sum_a \text{Tr} [C_{R2}^a(q_2) (C_{R2}^a(q'_{2\perp}))^\dagger] \\ &= C_F \int \frac{d^2x d^2y d^2x' d^2y'}{(2\pi)^6} e^{-i(K+k_{\bar{q}}) \cdot (x-x')} e^{iq_2 \cdot (x-y)} e^{-iq'_{2\perp} \cdot (x'-y')} \\ &\quad \times \text{Tr} \{ [V(x) V^\dagger(y) - \mathbb{1}] [V(y') V^\dagger(x') - \mathbb{1}] \}. \end{aligned} \quad (122)$$

It is straightforward, albeit tedious, to compute the perturbative factor $\mathcal{H}^{\lambda}(q_2, q'_{2\perp})$ from the explicit expressions for the \mathcal{J} given by Eq. (110) in the longitudinally polarized case and Eqs. (111)-(112) in the transversely polarized case. In these expressions, the change of variable from $z_{\bar{q}}$ to ξ enables one to get rid off the hard scale dependence from the light-cone energy denominators, such that this dependence factorise in the final result:

$$\mathcal{H}^{\lambda}(q_2, q'_{2\perp}) = H^{\lambda}(z_q, Q^2, P) \times \frac{2K^2 (q_2 - k_{\bar{q}}) \cdot (q'_{2\perp} - k_{\bar{q}})}{C_F [\xi K^2 + (1 - \xi)(q_2 - k_{\bar{q}})^2] [\xi K^2 + (1 - \xi)(q'_{2\perp} - k_{\bar{q}})^2]}. \quad (123)$$

Here, the hard scale dependence only appears in $H^\lambda(z_q, Q^2, \mathbf{P})$ given by

$$H^{\lambda=0}(z_q, Q^2, \mathbf{P}) = \alpha_s C_F \alpha_{em} e_f^2 \delta(1 - z_q - z_g) \frac{8Q^2 z_q^3 z_g^2}{[z_q z_g Q^2 + \mathbf{P}^2]^3}, \quad (124)$$

$$H^{\lambda=\pm 1}(z_q, Q^2, \mathbf{P}) = \alpha_s C_F \alpha_{em} e_f^2 \delta(1 - z_q - z_g) \frac{2z_q \left\{ [\mathbf{P}^2 + z_q z_g Q^2]^2 + z_g^2 (\mathbf{P})^4 + z_q^4 z_g^2 Q^2 \right\}}{\mathbf{P}^2 [z_q z_g Q^2 + \mathbf{P}^2]^3}. \quad (125)$$

In the transversely polarized case, we also *average* over the two polarizations of the virtual photon. One recognizes in these two expressions the standard LO hard factors for the $2 \rightarrow 2$ scattering process $\gamma^* + q \rightarrow q + g$ as obtained in collinear factorization. They are identical to the hard factors for the corresponding diffractive process previously computed from the CGC in [24].

Integrating over the soft antiquark transverse momentum

We now turn to the integration over the unmeasured soft-antiquark, and in particular to the integrating over its transverse momentum $\mathbf{k}_{\bar{q}}$ which simplifies the color operator at the cross-section level given by Eq. (122). In order to integrate over $\mathbf{k}_{\bar{q}}$, let us perform the change of variables

$$\mathbf{q}_2 \rightarrow -\mathbf{q} + \mathbf{k}_{\bar{q}} + \mathbf{K}, \quad \mathbf{q}'_{2\perp} \rightarrow -\mathbf{q}' + \mathbf{k}_{\bar{q}} + \mathbf{K}, \quad (126)$$

so that the dependence on $\mathbf{k}_{\bar{q}}$ disappears from the perturbative factor Eq. (123) and is now fully contained in the color correlator Ξ , for which we give an explicit expression below:

$$\begin{aligned} \Xi(-\mathbf{q} + \mathbf{k}_{\bar{q}} + \mathbf{K}, -\mathbf{q}' + \mathbf{k}_{\bar{q}} + \mathbf{K}) &= C_F \int \frac{d^2 \mathbf{x} d^2 \mathbf{y} d^2 \mathbf{x}' d^2 \mathbf{y}'}{(2\pi)^6} e^{-i\mathbf{k}_{\bar{q}} \cdot (\mathbf{y} - \mathbf{y}')} e^{-i\mathbf{q} \cdot (\mathbf{x} - \mathbf{y})} e^{i\mathbf{q}' \cdot (\mathbf{x}' - \mathbf{y}')} \\ &\times e^{-i\mathbf{K} \cdot (\mathbf{y} - \mathbf{y}')} \text{Tr} \left\{ [V(\mathbf{x}) V^\dagger(\mathbf{y}) - \mathbb{1}] [V(\mathbf{y}') V^\dagger(\mathbf{x}') - \mathbb{1}] \right\}. \end{aligned} \quad (127)$$

Let us now integrate the correlator:

$$\begin{aligned} &\int d^2 \mathbf{k}_{\bar{q}} \Xi(-\mathbf{q} + \mathbf{k}_{\bar{q}} + \mathbf{K}, -\mathbf{q}' + \mathbf{k}_{\bar{q}} + \mathbf{K}) \\ &= C_F \int \frac{d^2 \mathbf{x} d^2 \mathbf{y} d^2 \mathbf{x}' d^2 \mathbf{y}'}{(2\pi)^4} e^{-i\mathbf{q} \cdot (\mathbf{x} - \mathbf{y})} e^{i\mathbf{q}' \cdot (\mathbf{x}' - \mathbf{y}')} \text{Tr} \left\{ [V(\mathbf{x}) V^\dagger(\mathbf{y}) - \mathbb{1}] [V(\mathbf{y}') V^\dagger(\mathbf{x}') - \mathbb{1}] \right\} \end{aligned} \quad (128)$$

$$\begin{aligned} &= C_F N_c \int d^2 \mathbf{b} \left[\mathcal{D}_F^{(1)}(\mathbf{b}, \mathbf{q}) \delta^{(2)}(\mathbf{q} - \mathbf{q}') - \mathcal{D}_F^{(1)}(\mathbf{b}, \mathbf{q}') \delta^{(2)}(\mathbf{q}) \right. \\ &\quad \left. - \mathcal{D}_F^{(1)}(\mathbf{b}, \mathbf{q}) \delta^{(2)}(\mathbf{q}') + \delta^{(2)}(\mathbf{q}) \delta^{(2)}(\mathbf{q}') \right], \end{aligned} \quad (129)$$

where \mathbf{b} is the impact parameter variable and its integration gives rise to an overall transverse area factor. As in the main text, we have defined the generalized dipole operator in momentum space as

$$\mathcal{D}_F^{(n)}(\mathbf{b}, \mathbf{q}) \equiv \int d^2 \mathbf{r} \frac{e^{-i\mathbf{q} \cdot \mathbf{r}}}{(2\pi)^2} \left(\frac{1}{N_c} \text{Tr} [V_{\mathbf{b}+\mathbf{r}/2} V_{\mathbf{b}-\mathbf{r}/2}^\dagger] \right)^n. \quad (130)$$

Final result for the TMD factorised cross-section

Combining Eqs. (120), (123) and (129) we finally find the TMD factorised result

$$\frac{d\sigma_{\gamma^* A \rightarrow qg+X}}{d^2 \mathbf{P} d^2 \mathbf{K} dz_g dz_q} = H^\lambda(z_q, Q^2, \mathbf{P}) \times xq^{(1)}(x, \mathbf{K}), \quad (131)$$

where the hard factors are given by Eqs. (124)-(125) and where the small- x sea quark TMD is given by

$$xq^{(1)}(x, \mathbf{K}) = \frac{N_c}{8\pi^4} \int_0^1 d\xi \int d^2b d^2q \left\langle \mathcal{D}_F^{(1)}(\mathbf{b}, \mathbf{q}) \right\rangle_{x/\xi} \times \left\{ 1 - \frac{2\mathbf{K} \cdot (\mathbf{K} - \mathbf{q})}{[\xi \mathbf{K}^2 + (1 - \xi)(\mathbf{K} - \mathbf{q})^2]} + \frac{(\mathbf{q} - \mathbf{K})^2 \mathbf{K}^2}{[\xi \mathbf{K}^2 + (1 - \xi)(\mathbf{K} - \mathbf{q})^2]^2} \right\}, \quad (132)$$

$$= \int_0^1 d\xi \int d^2q \frac{x}{\xi} G^{(2)}\left(\frac{x}{\xi}, \mathbf{q}\right) \times \frac{\alpha_s}{(2\pi)^2} \frac{1}{q_\perp^2} \left\{ 1 - \frac{2\mathbf{K} \cdot (\mathbf{K} - \mathbf{q})}{[\xi \mathbf{K}^2 + (1 - \xi)(\mathbf{K} - \mathbf{q})^2]} + \frac{(\mathbf{q} - \mathbf{K})^2 \mathbf{K}^2}{[\xi \mathbf{K}^2 + (1 - \xi)(\mathbf{K} - \mathbf{q})^2]^2} \right\}, \quad (133)$$

with the dipole gluon TMD $xG^{(2)}$ defined as

$$xG^{(2)}(x, \mathbf{q}) = \frac{q_\perp^2 N_c}{2\pi^2 \alpha_s} \int d^2b \left\langle \mathcal{D}_F^{(1)}(\mathbf{b}, \mathbf{q}) \right\rangle_x. \quad (134)$$

If one neglects the dependence upon the integration variable ξ in the dipole gluon TMD in Eq. (133) using $\frac{x}{\xi} G^{(2)}(x/\xi, \mathbf{q}) \approx xG^{(2)}(x, \mathbf{q})$, the ξ integral can be performed analytically yielding

$$xq^{(1)}(x, \mathbf{K}) = \frac{N_c}{4\pi^4} \int d^2b d^2q \left\langle \mathcal{D}_F^{(1)}(\mathbf{b}, \mathbf{q}) \right\rangle_x \left\{ 1 - \frac{\mathbf{K} \cdot (\mathbf{K} - \mathbf{q})}{K_\perp^2 - (\mathbf{K} - \mathbf{q})^2} \ln \left(\frac{K_\perp^2}{(\mathbf{K} - \mathbf{q})^2} \right) \right\}, \quad (135)$$

in agreement with the result provided in the main text of the Letter.

Differential cross-section for inclusive quark-gluon dijet in gluon-initiated proton-nucleus collisions

In this section, we provide the results for the leading power contribution to the amplitude and the differential cross-section for inclusive gluon-quark dijets in gluon-initiated pA collisions. The results are obtained following the strategy of the previous sections, the details along with the computation for other dijet channels in pA will be provided in forthcoming work.

The total amplitude receives contributions from 9 diagrams as shown in Fig.8, which can be classified into three types according to the gluon emitter: quark ($f = q$), antiquark ($f = \bar{q}$), or gluon ($f = g$) parent. At LP in K_\perp/P_\perp and Q_s/P_\perp the total amplitude reads:

$$\mathcal{M}_{qg(\bar{q}), \sigma\bar{\sigma}, i\bar{i}}^{\lambda\bar{\lambda}, ab} = 8g^2 q^+ \sqrt{z_q z_{\bar{q}}} \frac{\mathbf{P}^k}{\mathbf{P}^2} \sum_{f=q, \bar{q}, g} \Gamma_{f, \sigma\bar{\sigma}}^{\lambda\bar{\lambda}, jk} \int \frac{d^2\ell}{(2\pi)^2} \mathcal{C}_{f, i\bar{i}}^{ab}(\mathbf{K} - \ell, \ell + \mathbf{k}_{\bar{q}}) \frac{\ell^j}{z_{\bar{q}} M_{qg}^2 + \ell^2}, \quad (136)$$

where $\sigma, \bar{\sigma}, \lambda, \bar{\lambda}$ respectively refer to the incoming and outgoing quark helicities and the incoming and outgoing gluon polarisations, and i, \bar{i}, a, b to the colors of quark, antiquark, and incoming and outgoing gluons. j, k are transverse indices and M_{qg} is the invariant mass of the qg -dijet. The corresponding splitting functions are:

$$\begin{aligned} \Gamma_{q, \sigma\bar{\sigma}}^{\lambda\bar{\lambda}, jk} &= -\delta^{\sigma, -\bar{\sigma}} \delta^{\sigma, -\lambda} (\delta^{\lambda, \bar{\lambda}} + z_q \delta^{\lambda, -\bar{\lambda}}) \epsilon^{\bar{\lambda}, k} \epsilon^{\lambda, j}, \\ \Gamma_{\bar{q}, \sigma\bar{\sigma}}^{\lambda\bar{\lambda}, jk} &= -\delta^{\sigma, -\bar{\sigma}} \delta^{\sigma, \bar{\lambda}} (z_g \delta^{\lambda, \bar{\lambda}} - z_q \delta^{\lambda, -\bar{\lambda}}) \epsilon^{\lambda, k} \epsilon^{\bar{\lambda}, j}, \\ \Gamma_{g, \sigma\bar{\sigma}}^{\lambda\bar{\lambda}, jk} &= z_g \delta^{\sigma, -\bar{\sigma}} \left[\frac{\delta^{\lambda, \bar{\lambda}} \epsilon^{\sigma, k}}{z_q} + \frac{\delta^{\lambda, -\sigma} \epsilon^{\bar{\lambda}, k}}{z_g} - \delta^{\bar{\lambda}, \sigma} \epsilon^{\lambda, k} \right] \epsilon^{\sigma, j}, \end{aligned} \quad (137)$$

and the color operators

$$\begin{aligned} \mathcal{C}_{q, i\bar{i}}^{ab}(\mathbf{q}_1, \mathbf{q}_2) &= \int_{\mathbf{x}, \mathbf{y}} e^{-i\mathbf{q}_1 \cdot \mathbf{x}} e^{-i\mathbf{q}_2 \cdot \mathbf{y}} [t^b V_{\mathbf{x}} t^a V_{\mathbf{y}}^\dagger - U_{\mathbf{x}}^{ca} t^b t^c], \\ \mathcal{C}_{\bar{q}, i\bar{i}}^{ab}(\mathbf{q}_1, \mathbf{q}_2) &= \int_{\mathbf{x}, \mathbf{y}} e^{-i\mathbf{q}_1 \cdot \mathbf{x}} e^{-i\mathbf{q}_2 \cdot \mathbf{y}} [U_{\mathbf{x}}^{bc} V_{\mathbf{x}} t^a t^c V_{\mathbf{y}}^\dagger - U_{\mathbf{x}}^{ca} t^c t^b], \\ \mathcal{C}_{g, i\bar{i}}^{ab}(\mathbf{q}_1, \mathbf{q}_2) &= \mathcal{C}_{q, i\bar{i}}^{ab}(\mathbf{q}_1, \mathbf{q}_2) - \mathcal{C}_{\bar{q}, i\bar{i}}^{ab}(\mathbf{q}_1, \mathbf{q}_2). \end{aligned} \quad (138)$$

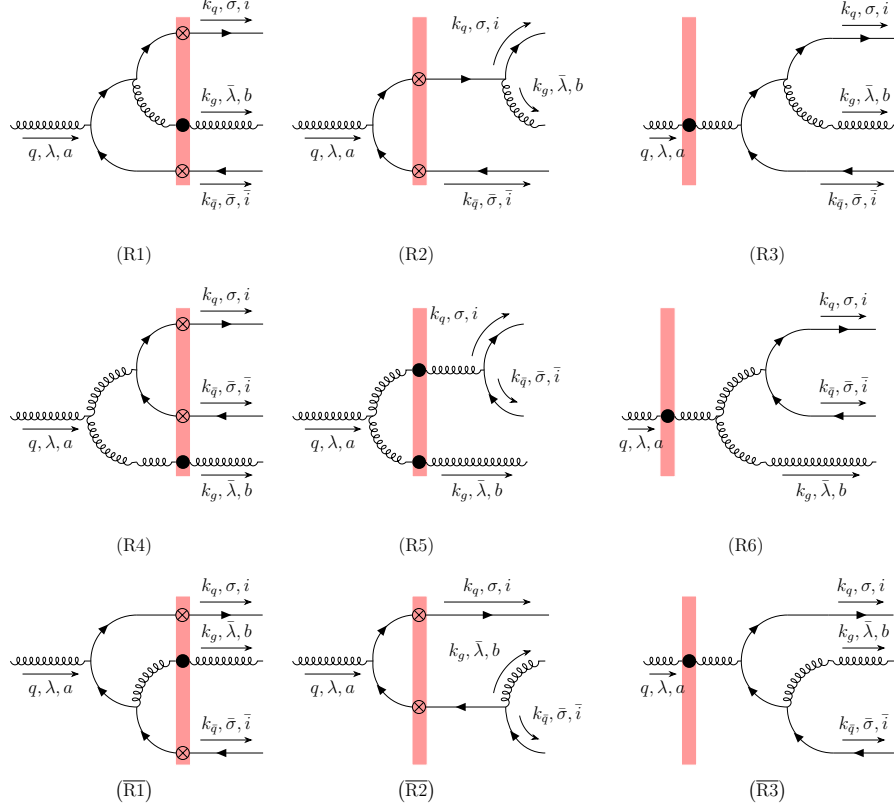


Figure 8. The nine diagrams contributing to $q\bar{q}g$ production in pA scattering in the CGC picture. The top three diagrams correspond to gluon emission from a quark. Middle diagrams correspond to gluon emission by gluon. Finally, the three diagrams in the bottom correspond to gluon emission from the antiquark.

The contributions coming from gluon emission from quark and gluon emission from antiquark are analogous to those in the qg jets in DIS. The splitting functions Γ_q and $\Gamma_{\bar{q}}$ are the same, while the color operators are different due to the color of the incoming gluon. The contribution from gluon emission from gluon is a new feature of this channel. Note that the color operator for the gluon emission from gluon can be written in terms of those for gluon emission from quark and antiquark as anticipated from our heuristic discussion at large N_c (cf. Fig. (5) in the main text).

Squaring this amplitude, integrating over the phase space of the antiquark ($z_{\bar{q}}, \mathbf{k}_{\bar{q}}$), and taking the large N_c limit, we find the differential cross-section

$$\frac{d\sigma_{gA \rightarrow gq+X}}{d^2\mathbf{P} d^2\mathbf{K} dz_q dz_g} = \delta(1 - z_q - z_g) \frac{\alpha_s^2 (1 + z_g^2)}{2z_q \mathbf{P}^4} \left[xq^{(3)}(x, \mathbf{K}) + z_g^2 xq^{(2)}(x, \mathbf{K}) \right], \quad (139)$$

where the quark TMDs are defined as

$$xq^{(n)}(x, \mathbf{K}) = \int_{\mathbf{b}, \mathbf{q}} \left\langle \mathcal{D}_F^{(n-1)}(\mathbf{b}, \mathbf{q}) \mathcal{Q}(\mathbf{b}, \mathbf{K} - \mathbf{q}) \right\rangle_x, \quad (140)$$

and we introduced the Fourier transform of the n^{th} power of the dipole correlator

$$\mathcal{D}_F^{(n)}(\mathbf{b}, \mathbf{q}) \equiv \int d^2\mathbf{r} \frac{e^{-i\mathbf{q} \cdot \mathbf{r}}}{(2\pi)^2} \left(\frac{1}{N_c} \text{Tr} \left[V_{\mathbf{b}+\mathbf{r}/2} V_{\mathbf{b}-\mathbf{r}/2}^\dagger \right] \right)^n. \quad (141)$$